

POLITECNICO DI TORINO

MASTER'S DEGREE
IN AEROSPACE ENGINEERING

Final Degree Project

Quasi-optimal low-thrust orbit transfers
using simplified steering laws



Tutors

Prof. Manuela BATTIPEDE

Prof. Jesús PELÁEZ ÁLVAREZ

Supervisor

Prof. Elena FANTINO

Author

Francesco GIANOTTO

September 2018

Politecnico di Torino
Dipartimento di Ingegneria Meccanica e Aerospaziale

Aerospace Engineering

Abstract

Quasi-optimal low-thrust orbit transfers using simplified steering laws

by Francesco GIANOTTO

As low-thrust manoeuvres are assuming more importance in spacecraft propulsion, the analysis of this kind of transfer is essential for its understanding and control. In this sense, we want to study simplified steering laws that are easier to perform with spacecrafts and that we can control in each point of the transfer. The analysis starts with Lagrange planetary equations applied with four steering laws and in case of periapsis or apoapsis centred burns, obtaining the Keplerian orbital elements' rates of change in one revolution. One of the most important applications of this method concerns the Jupiter's moons tour, a tour between the Galilean moons that nowadays is the subject of many studies. Therefore, we analyse the coplanar transfer between two Galilean moons, using the four steering laws, including combinations of them, and developing algorithms in order to optimize the transfer. The benefit of using this method is given by the direct control over the generated algorithms and the geometrical understanding of the entire transfer.

The last part of this thesis deals with the singularity that affects the Lagrange planetary equations, with its inclination equal to zero. The innovative and central point for the resolution is that the inclination is not a geometrical element that characterizes the orbit, but it depends on the reference frame used. Thus, applying a rotation of the reference frame we can resolve the singularity without having to rely on the equinoctial elements, the use of which leads to several complications.

Acknowledgements

I want to thank all those who helped me in carrying out this thesis.

First of all, this work would not have been possible without the support of my family and my friends during all these years.

I would like to express my very great appreciation to Professor Elena Fantino, my supervisor, for her patient guidance and her precious advice. Her help has been fundamental for the success of this thesis.

I am also incredibly thankful to Professor Jesús Peláez Álvarez for his helpfulness, and to Professor Manuela Battipede, whose passion in her lessons gave me inspiration.

Contents

Abstract	ii
Acknowledgements	iii
Contents	iv
List of Figures	vi
List of Tables	vii
Introduction	ix
1 Low-thrust transfer with simplified steering laws	1
1.1 Model description	1
1.2 Rates of change in one revolution	5
1.2.1 Steering law (1)	6
1.2.2 Steering law (2)	6
1.2.3 Steering law (3)	7
1.2.4 Steering law (4)	7
1.2.5 Application for GTO	7
1.3 Secular rates of change	10
1.3.1 Steering law (1)	10
1.3.2 Steering law (2)	11
1.3.3 Steering law (3)	11
1.3.4 Steering law (4)	11
1.4 Application of GTO-to-GEO transfer	12
2 Jupiter's moons coplanar transfer	15
2.1 Jupiter's moons tour	15
2.2 Europa-Ganymede coplanar transfer	16
2.2.1 Jupiter secular rates of change	17
2.2.2 Jupiter rates of change in one revolution	19
2.3 Orbit transfer with single thrust mode	20
2.3.1 Burn angle and number of revolutions for the single thrust mode	20
2.3.2 Delta V and total time for the single thrust mode	21
2.4 Comparison of average and updated values	23
2.5 Orbit transfer with double thrust mode	24

2.6	Propellant mass	27
3	Singular case of inclination zero	28
3.1	From state vector to orbital elements	28
3.2	From orbital elements to state vector	30
3.3	Application of inclination = 0	31
	Conclusion	34
A	Operations for secular rates equations	36
A.1	Case 1	36
A.1.1	Semi-major axis $\frac{da}{dE}$	36
A.1.2	Eccentricity $\frac{de}{dE}$	37
A.1.3	Inclination $\frac{di}{dE}$	38
A.1.4	RAAN $\frac{d\Omega}{dE}$	38
A.1.5	Argument of periapsis $\frac{d\omega}{dE}$	39
A.2	Case 2	40
A.2.1	Semi-major axis $\frac{da}{dE}$	40
A.2.2	Eccentricity $\frac{de}{dE}$	41
A.2.3	Inclination $\frac{di}{dE}$	41
A.2.4	RAAN $\frac{d\Omega}{dE}$	41
A.2.5	Argument of periapsis $\frac{d\omega}{dE}$	42
A.3	Case 3	42
A.3.1	Semi-major axis $\frac{da}{dE}$	42
A.3.2	Eccentricity $\frac{de}{dE}$	43
A.3.3	Inclination $\frac{di}{dE}$	44
A.3.4	RAAN $\frac{d\Omega}{dE}$	44
A.3.5	Argument of periapsis $\frac{d\omega}{dE}$	44
A.4	Case 4	45
A.4.1	Semi-major axis $\frac{da}{dE}$	45
A.4.2	Eccentricity $\frac{de}{dE}$	45
A.4.3	Inclination $\frac{di}{dE}$	46
A.4.4	RAAN $\frac{d\Omega}{dE}$	46
A.4.5	Argument of periapsis $\frac{d\omega}{dE}$	46
	Bibliography	48

List of Figures

1.1	Reference systems and orbital elements	3
1.2	Simplified steering laws	4
1.3	Burn arc and burn angle	5
1.4	Rates of change in one revolution of a and e for cases (1), (2) and (3), in GTO orbit	8
1.5	Rates of change in one revolution of i and Ω , in GTO orbit	9
1.6	Rates of change in one revolution of ω , in GTO orbit [left: cases (1) (2) (3); right: case (4)]	9
1.7	Rate of change in one revolution of ΔV , in GTO orbit	10
1.8	Secular rates of a and e for steering laws (1) (2) and (3), in Earth orbit	12
1.9	Evolution of a , e (left) and i (right) for a GTO-GEO transfer	13
2.1	Secular rates of a and e for different cases, initial orbit around Jupiter	18
2.2	Rates of change of a and e in one revolution, average orbit around Jupiter	19
2.3	Δa_{tot} (left) and Δe_{tot} (right) as functions of burn arc and number of revolutions, periapsis burn, steering law (1)	21
2.4	Graphs of Δa_{req} and Δe_{req} for single thrust mode	22
2.5	Δa_{tot} (left) and Δe_{tot} (right) as functions of burn arc and number of revolutions, periapsis burn, steering law (1)	23
2.6	Total ΔV in function of burn angles for double thrust mode	26
2.7	Total time in function of burn angles for double thrust mode	26
3.1	Reference system for an orbit with $i = 0$	32

List of Tables

1.1	Cases for in-plane acceleration.	4
1.2	GTO-GEO data	13
2.1	Jupiter's orbits data	16
2.2	Results of burn angle and number of revolutions for single thrust mode	21
2.3	Results of ΔV and total time for single thrust mode	22
2.4	Comparison results of burn angle and number of revolutions for single thrust mode	24
2.5	Comparison results of ΔV and total time for single thrust mode	24
2.6	Minimum ΔV and minimum total time for double thrust mode	25
3.1	Orbit data after the rotation	32

Introduction

Referring to space propulsion, nowadays there are two mostly used types of propulsion systems. The first one is chemical propulsion and it is characterized by high thrust and low specific impulse. It is used for impulsive manoeuvres for which the burn time tends to zero and it is the only propulsion system available for the launch. In general, it is preferred in missions where the ΔV budget is not too high. The second one is electric propulsion, characterized by low thrust and high specific impulse. It allows performing a transfer with less propellant compared to the same transfer performed with an impulsive manoeuvre. Nevertheless, it requires more time to complete the manoeuvre due to longer trajectories.

Nowadays, low-thrust transfers are used in a broad spectrum of contexts, both in planetary and interplanetary orbits, the latter one performed together with gravity assist (Schutze et al.^[1], 2009). The transfer between two circular and coplanar orbits can be obtained with a tangential thrust that generates a spiral trajectory (Edelbaum^[2], 1961). The same transfer performed with impulsive burns could be achieved with the Hohmann transfer, a highly elliptical orbit tangent to the two circular orbits. The typical ΔV s for a LEO-to-GEO transfer are about 6 km/s for the low-thrust and 3.5 km/s for the Hohmann transfer. Even if ΔV is higher in the first case, the benefits of less propellant derive from the electric thruster's higher efficiency. Considering a specific impulse of respectively 3000 s and 400 s, the propellant mass for the impulsive manoeuvre is about 6 times bigger than the propellant for the low-thrust transfer.

A limitation of the electric thruster is the high power requested. Therefore, for a deep space mission this method of propulsion could not be appropriate. Nevertheless, the technology of these thrusters is constantly evolving, allowing missions as Deep Space 1 to use an ion propulsion system (NSTAR) for the primary manoeuvres (Polk et al.^[3], 2001). Nowadays, NASA has developed the ion thruster NEXT, more powerful and efficient than NSTAR (Schmidt^[4],

2008), and there are many studies about electric propulsion for small satellite missions (Manente et al.^[5], 2017).

The difficulty of designing a mission with low-thrust transfer is based on finding the best way to perform the thrust. In fact, the problem is based on optimal control, thus on optimization with constraints on the time or on the path. The first results were given by Bryson and Ho^[6] (1975), applying an optimization to find the angle of thrust along the entire path for different problems, as circle-to-circle transfer or orbit injection. Nowadays, there are several methods of optimization for a wide range of problems (Conway^[7], 2010), but it is not always simple to solve them.

It is also interesting to analyse the consequence of using simple steering laws, the subject of this thesis. In fact, it is often the only way to perform the transfer due to spacecraft imposed constraints. The current technology does not allow performing too complex manoeuvres, especially considering the needs of the other spacecraft subsystems. For example, we can think about the impossibility to control directly the spacecraft's manoeuvres in a deep space mission, because of the distance from the Earth. Therefore, the study of these simplified steering laws, alone or in combination, is important for its current applications. Furthermore, it allows having a geometrical understanding of the problem, contrary to a toolbox of optimal control on which we do not have direct control.

The developed model for the analysis of these simplified steering laws is based on the Lagrange planetary equations. Integrating them, we obtain the rates of change of the orbital elements as functions of the steering laws and the burn angle. These results can be used for several problems, such as the Jupiter's moons tour. Nowadays, space agencies are able to send spacecrafts orbiting the giants planets, and the scientific community has great interest in studying its moons' systems. Due to chemical thrusters performance, each transfer of a moons' tour has a high cost of propellant. Thus, in order to perform an entire tour, it is necessary to use low-thrust manoeuvres or transfer with gravity assists. This thesis takes into account the first method of low-thrust manoeuvres. In order to reduce the amount of propellant needed, we consider a low-energy transfer as presented by Fantino and Castelli^[8] (2016), but considering a low-thrust transfer instead of impulsive transfer in the central part of the manoeuvre.

Nevertheless, the Lagrange planetary equations used in this model have a singularity for inclination equal to zero. This singularity does not allow applying this model to a wide range of problems. The original solution described in this thesis derives from the analysis of the properties of inclination. The key point consists in a rotation of the reference frame, as the

real problem does not lie in the orbital elements, but in an inappropriate reference frame choice.

The following part of this thesis is organized as follows:

- Chapter 1 describes the model for performing a low-thrust transfer using simplified steering laws. It is based on the analysis of Pollard^[9] (1997), and it presents applications for a GTO-to-GEO transfer.
- Chapter 2 deals with the coplanar transfer between the two moons of Jupiter, Europa and Ganymede, using the model of the first chapter. It is based on the work of Fantino and Castelli^[8] (2016), and it can be included in the Jupiter's moons tour. The transfer is analysed above different aspects in order to find the best one.
- Chapter 3 presents a solution for solving the singular case of inclination equal to zero, which affects the Lagrange planetary equations. This solution allows us to use this model and in general the Lagrange equations for each kind of transfer.

The thesis ends with the Appendix A where the operations of the model presented in the first chapter are carried out.

Chapter 1

Low-thrust transfer with simplified steering laws

In this chapter we present the analysis of Pollard^[9] (1997) and Pollard^[10] (2000) (hereinafter, POLLARD97 and POLLARD00 respectively). The method he presents allows us to calculate the variation of the orbital elements in case of a low-thrust manoeuvre, using four simple steering laws. It is based on the integration of the Gauss form of the Lagrange planetary equations, simplified thanks to the steering laws, which lead to the rates of change in one revolution and to the secular rates of change. These equations express the variation of the Keplerian orbital elements as function of the amount and direction of the thrust.

We apply this method to a very common orbit: the geostationary transfer orbit (GTO). It is a Hohmann transfer orbit used to reach the GEO orbit. It has high eccentricity and an apogee of 42164 km that corresponds to the geostationary altitude. Its inclination is due to the latitude of the launch site (28.5° for the Kennedy Space Center), and typically its perigee is few hundred kilometres above sea level. This values are normally chosen in order to minimize the launcher cost in term of ΔV .

1.1 Model description

Thanks to developments in electrical propulsion, low-thrust orbit transfers are nowadays becoming more interesting for many applications. Unlike impulsive manoeuvres, in order to achieve a real benefit in term of used propellant, we have to control the intensity and the

direction of the thrust. We can achieve this goal by using optimal control, but it requires large computing skills, and it is often impossible to realize those manoeuvres due to practical constraints of the spacecraft.

A way to simplify the problem is given by POLLARD97 and POLLARD00 using simple steering laws that allow us to obtain the solution with an analytic method and easier calculations. An example of the validity of this method is the transfer between two circular and coplanar orbits. In this case, we know that the optimal thrust for achieving the minor ΔV is tangent to the orbit, and Pollard's method gives the same result.

According to Pollard, we will use the geocentric equatorial coordinate system shown in Fig. 1.1, with the unit vector \hat{I} in the plane of the Earth's equator and toward the vernal equinox, the unit vector \hat{J} in the same plane with 90° to the east, and the unit vector \hat{K} along the north polar axis. In addition to this, we will use a reference frame centred in the spacecraft for the three components of the velocity: V_r in the direction of the radius vector, V_t in the orbit plane and normal to the radius vector, V_n normal to the orbit plane in the direction of the angular momentum vector. One of the components of acceleration f , respectively f_1 f_2 f_3 , is associated to each velocity component, with the same reference frame. In this analysis we will use and calculate the variation of the Keplerian orbital elements: semi-major axis a , eccentricity e , inclination i , right ascension of the ascending node (RAAN) Ω , and the argument of periaxis ω . In Fig. 1.1 we show all the reference systems and the parameters used in this analysis, with the true anomaly expressed as ν .

We also report the Kepler's equation with the relation between the time t and the eccentric anomaly E that we will use in the next sections:

$$t = \sqrt{\frac{a^3}{\mu}} (E - e \sin E) \quad (1.1)$$

The analysis starts with the Gauss form of Lagrange planetary equations, expressed as functions of E , as presented by Burt^[11] (1967). In fact, we do not want to study the variations of the orbital elements as functions of time, but as functions of the burn angle, which is correlated to E . The mathematical operation applied in order to obtain these equations is simple: $\frac{dx}{dE} = \frac{dx}{dt} \frac{dt}{dE}$, where x is any orbital element. Therefore, we have the following five equations:

$$\frac{da}{dE} = \frac{2a^3}{\mu} \left(f_1 e \sin E + f_2 \sqrt{1 - e^2} \right) \quad (1.2)$$

$$\frac{de}{dE} = \frac{a^2}{\mu} \left[f_1 (1 - e^2) \sin E + f_2 \sqrt{1 - e^2} (2 \cos E - e - e \cos^2 E) \right] \quad (1.3)$$

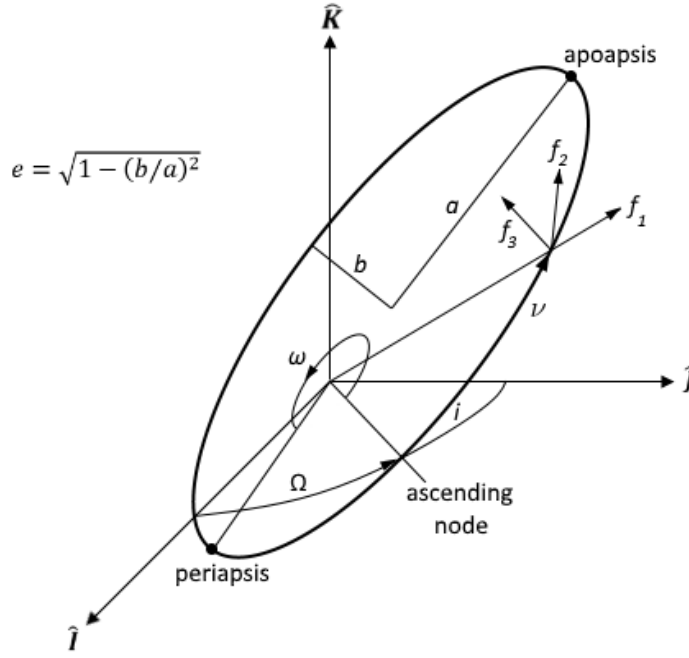


FIGURE 1.1: Reference systems and orbital elements

$$\frac{di}{dE} = \frac{a^2}{\mu} f_3 (1 - e \cos E) \left[\frac{(\cos E - e) \cos \omega}{\sqrt{1 - e^2}} - \sin E \sin \omega \right] \quad (1.4)$$

$$\frac{d\Omega}{dE} = \frac{a^2}{\mu} f_3 \frac{(1 - e \cos E)}{\sin i} \left[\frac{(\cos E - e) \sin \omega}{\sqrt{1 - e^2}} + \sin E \cos \omega \right] \quad (1.5)$$

$$\begin{aligned} \frac{d\omega}{dE} = \frac{a^2}{\mu} \left\{ \frac{1}{e} \left[-f_1 \sqrt{1 - e^2} (\cos E - e) + f_2 (2 - e^2 - e \cos E) \sin E \right] - \right. \\ \left. - f_3 (1 - e \cos E) \cot i \left[\frac{(\cos E - e) \sin \omega}{\sqrt{1 - e^2}} + \sin E \cos \omega \right] \right\} \quad (1.6) \end{aligned}$$

We can observe that a and e are affected by the in-plane accelerations f_1 and f_2 , while i and Ω by the out-of-plane acceleration f_3 , and ω is affected by all three components.

In order to solve these equations, we assume that the variation of each element during an orbit's single period is negligible. Hence, as for the integration step, we can keep constant each element for the duration of one revolution.

We will analyse four pitch steering laws (Fig. 1.2), considering a particular configuration for the two components of in-plane acceleration: (1) perpendicular to the orbit radius vector, (2) tangent to the orbit path, (3) perpendicular to the major axis of the ellipse, (4) parallel to the major axis of the ellipse. As a result of geometrical considerations for the above mentioned cases, we are able to obtain values for f_1 and f_2 , writing them as functions of E and f_{12} , where $f_{12} = \sqrt{(f_1)^2 + (f_2)^2} = f \cos \beta$, in Table 1.1.

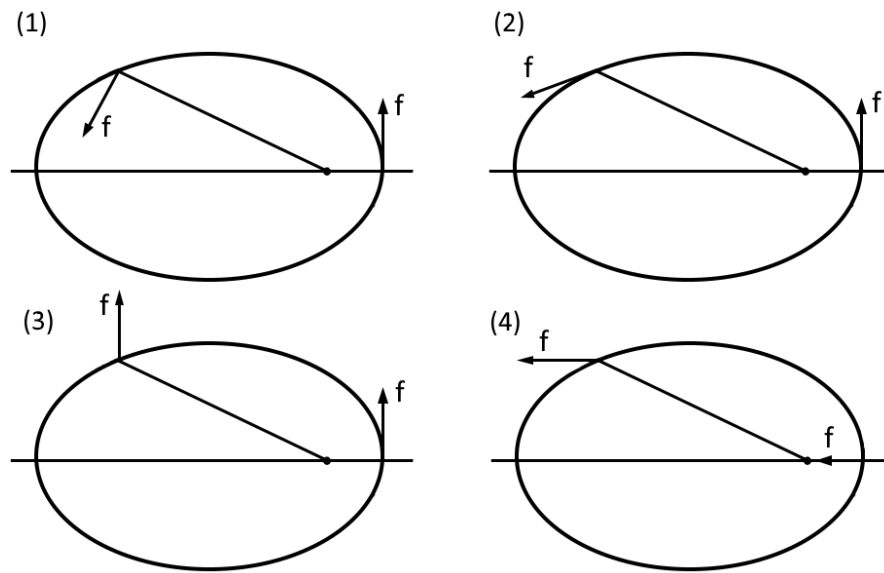


FIGURE 1.2: Simplified steering laws

TABLE 1.1: Cases for in-plane acceleration.

	$f_1(E)$	$f_2(E)$
Perpendicular to the orbit radius vector (1)	0	f_{12}
Tangent to the orbit path (2)	$\frac{f_{12} e \sin E}{\sqrt{1 - e^2 \cos^2 E}}$	$f_{12} \sqrt{\frac{1 - e^2}{1 - e^2 \cos^2 E}}$
Perpendicular to the major axis of the ellipse (3)	$\frac{f_{12} \sqrt{1 - e^2} \sin E}{1 - e \cos E}$	$\frac{f_{12} (\cos E - e)}{1 - e \cos E}$
Parallel to the major axis of the ellipse (4)	$\frac{f_{12} (\cos E - e)}{1 - e \cos E}$	$\frac{-f_{12} \sqrt{1 - e^2} \sin E}{1 - e \cos E}$

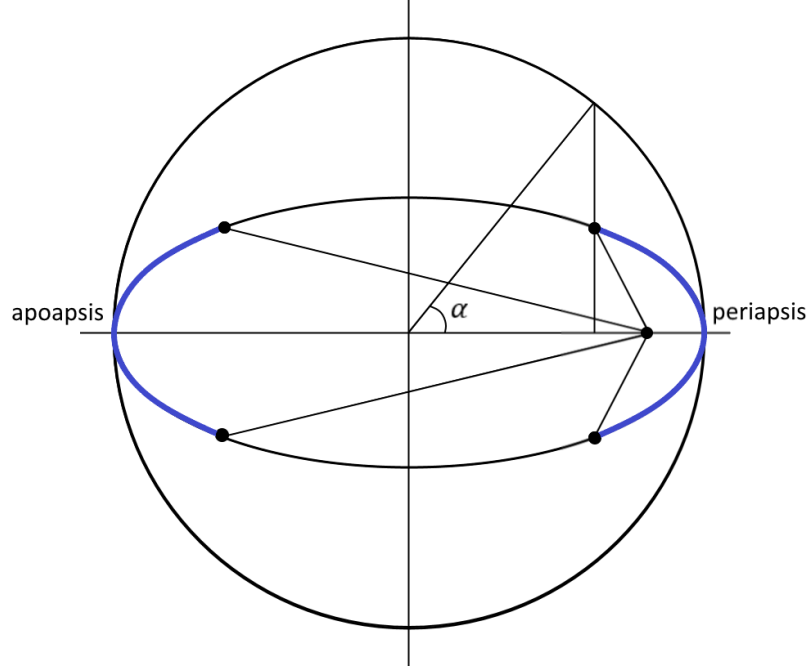


FIGURE 1.3: Burn arc and burn angle

1.2 Rates of change in one revolution

Integrating equations 1.2 to 1.6 over the burn arc and for the chosen steering law, we obtain the rates of change of the orbital elements in one revolution. We consider that the burn arcs are centred in periaapsis or apoapsis with the angle ranging respectively as $-\alpha \leq E \leq +\alpha$ or $(\pi - \alpha) \leq E \leq (\pi + \alpha)$, where α is the burn angle as shown in Fig. 1.3.

The complete operations are carried out and available in Appendix A. The results are summarised here, where apoapsis burns have $\sigma = 1$, periaapsis burns $\sigma = -1$, and the function G is:

$$G(\sigma, \alpha, e) = \frac{2\sigma \sin \alpha (1 + e^2) + 3e\alpha + e \cos \alpha \sin \alpha}{\sqrt{1 - e^2}} \quad (1.7)$$

We present also the rate of change of ΔV , useful in this analysis for the comparison with an impulsive transfer. It is obtained as $\Delta V = f \cdot t_{burn}$, where t_{burn} is the burn duration per revolution and its equation derives from the Kepler's equation 1.1:

$$t_{burn} = 2\sqrt{\frac{a^3}{\mu}}(\alpha + \sigma e \sin \alpha) \quad (1.8)$$

Unlike Pollard's analysis, for the sake of simplicity in the current model we do not consider the influence of the planet's oblateness (the J_2 factor) that partially affects the rates of change

of Ω and ω in case of low orbit. We also neglect all the other perturbations, such as moons' gravitation and solar pressure.

1.2.1 Steering law (1)

In steering law (1), the in-plane acceleration is perpendicular to the orbit radius vector. We obtain the following equations:

$$\Delta a = \frac{4a^3}{\mu} f_{12} \sqrt{1 - e^2} \alpha \quad (1.9)$$

$$\Delta e = -\frac{a^2}{\mu} f_{12} \sqrt{1 - e^2} (4\sigma \sin \alpha + 3e\alpha + e \sin \alpha \cos \alpha) \quad (1.10)$$

$$\Delta i = -\frac{a^2}{\mu} f_3 \cos \omega G(\sigma, \alpha, e) \quad (1.11)$$

$$\Delta \Omega = -\frac{a^2}{\mu} f_3 \frac{\sin \omega}{\sin i} G(\sigma, \alpha, e) \quad (1.12)$$

$$\Delta \omega = \frac{a^2}{\mu} f_3 \sin \omega \cot i G(\sigma, \alpha, e) \quad (1.13)$$

$$\Delta V = 2\sqrt{\frac{a^3}{\mu}} \sqrt{(f_{12})^2 + (f_3)^2} (\alpha + \sigma e \sin \alpha) \quad (1.14)$$

1.2.2 Steering law (2)

In steering law (2), the in-plane acceleration is tangent to the orbit path. We obtain the following equations:

$$\Delta a = \frac{4a^3}{\mu} f_{12} \int_0^\alpha \sqrt{1 - e^2 \cos^2 E} dE \quad (1.15)$$

$$\Delta e = \frac{4a^2}{\mu} f_{12} (1 - e^2) \int_0^\alpha \frac{\cos E (1 - e \cos E)}{\sqrt{1 - e^2 \cos^2 E}} dE \quad (1.16)$$

In case of apoapsis-centred burn, the limits of the integral are π and $\pi + \alpha$.

The expressions Δi , $\Delta \Omega$, $\Delta \omega$, ΔV are the same as in case (1).

1.2.3 Steering law (3)

In steering law (3), the in-plane acceleration is perpendicular to the major axis of the ellipse. We obtain the following equations:

$$\Delta a = -\frac{4\sigma a^3}{\mu} f_{12} \sqrt{1-e^2} \sin \alpha \quad (1.17)$$

$$\Delta e = \frac{a^2}{\mu} f_{12} \sqrt{1-e^2} (4\sigma e \sin \alpha + 3\alpha + \sin \alpha \cos \alpha) \quad (1.18)$$

The expressions Δi , $\Delta \Omega$, $\Delta \omega$, ΔV are the same as in case (1).

1.2.4 Steering law (4)

In steering law (4), the in-plane acceleration is parallel to the major axis of the ellipse. We obtain the following equations:

$$\Delta a = 0 \quad (1.19)$$

$$\Delta e = 0 \quad (1.20)$$

$$\Delta \omega = \frac{a^2}{\mu} \left[f_{12} \frac{\sqrt{1-e^2}}{e} (-2\sigma e \sin \alpha - 3\alpha + \sin \alpha \cos \alpha) + f_3 \sin \omega \cot i G(\sigma, \alpha, e) \right] \quad (1.21)$$

The expressions Δi , $\Delta \Omega$, ΔV are the same as in case (1).

1.2.5 Application for GTO

From the obtained equations, we can see that the component f_3 does not affect a and e , and the component f_{12} does not affect i and Ω . If we want to obtain the variations of i and Ω , we have to introduce the out-of-plane component f_3 . This component does not affect only i and Ω , but it alters the argument of periapsis ω too.

Considering a typical GTO with $a = 24364$ km, $e = 0.7306$, $i = 28.5^\circ$, $\omega = 30^\circ$ and considering a typical acceleration $f = 3 \cdot 10^{-7}$ km/s², composed by $f_{12} = f_3 = 2.1213 \cdot 10^{-7}$ km/s², we present the rates of change as functions of the normalized burn angle α/π . We use the standard gravitational parameter of the Earth $\mu_e = 398601$ km³/s². With these data, Fig. 1.4 shows the comparison for a and e between the first three steering laws and in case

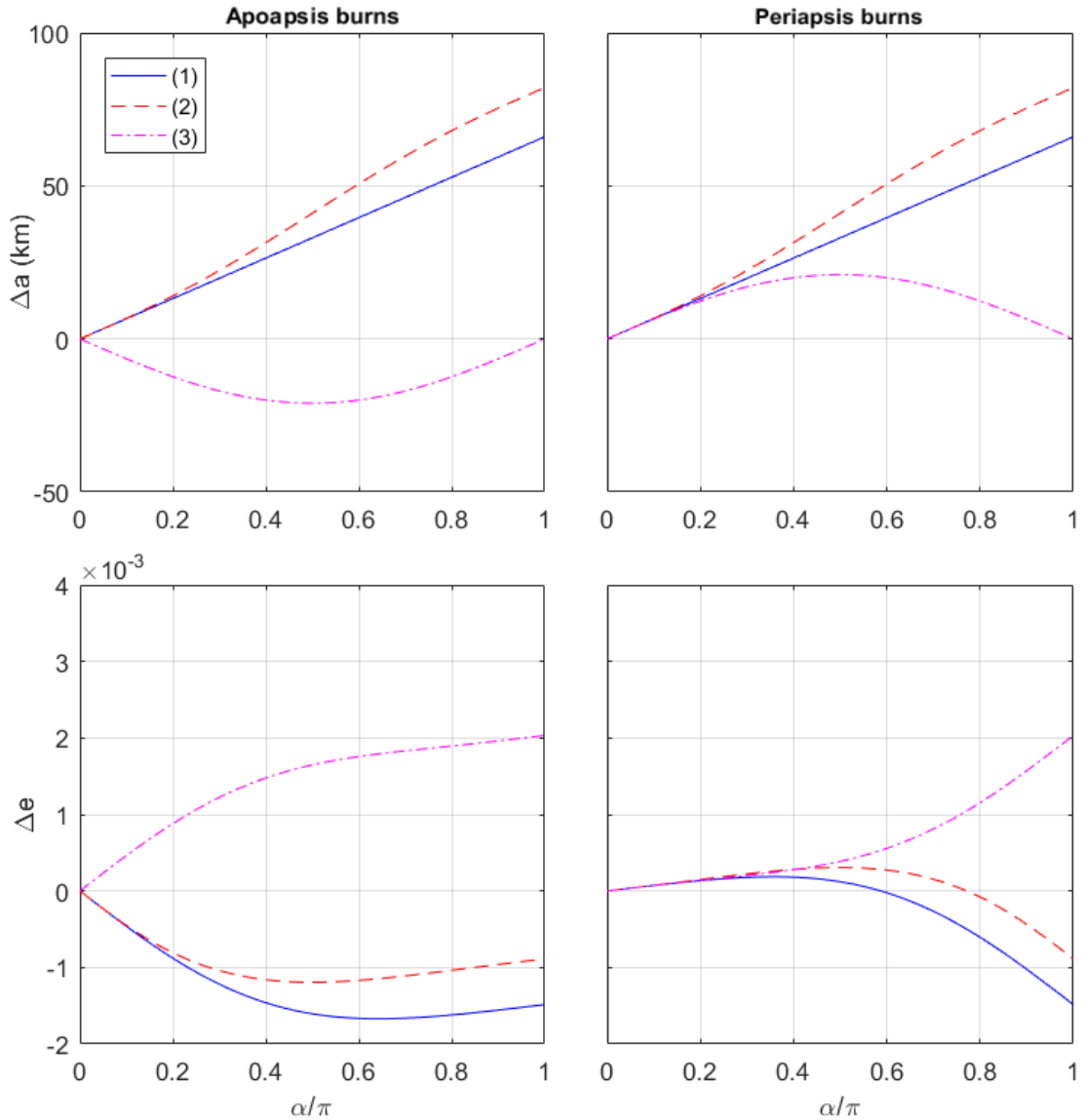
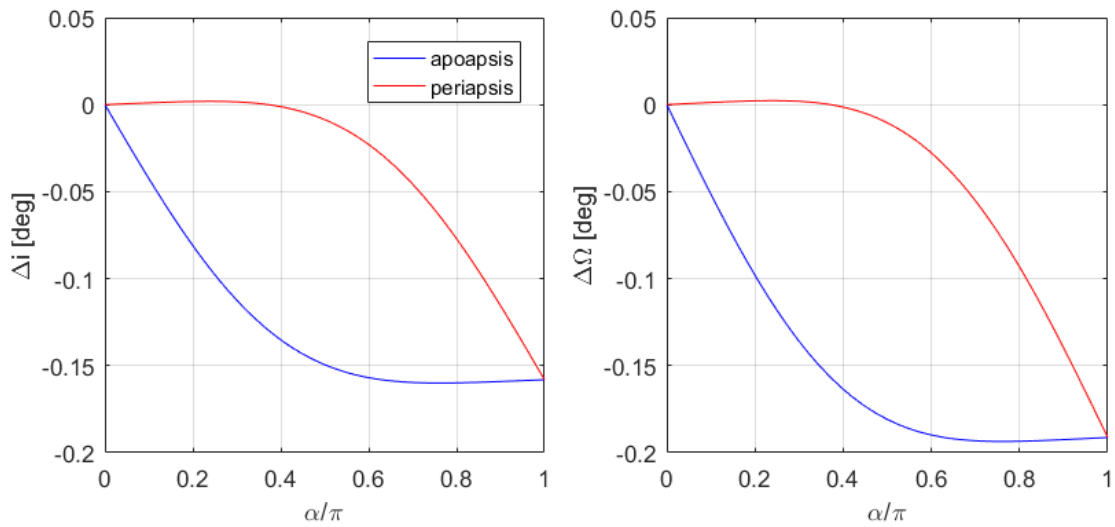
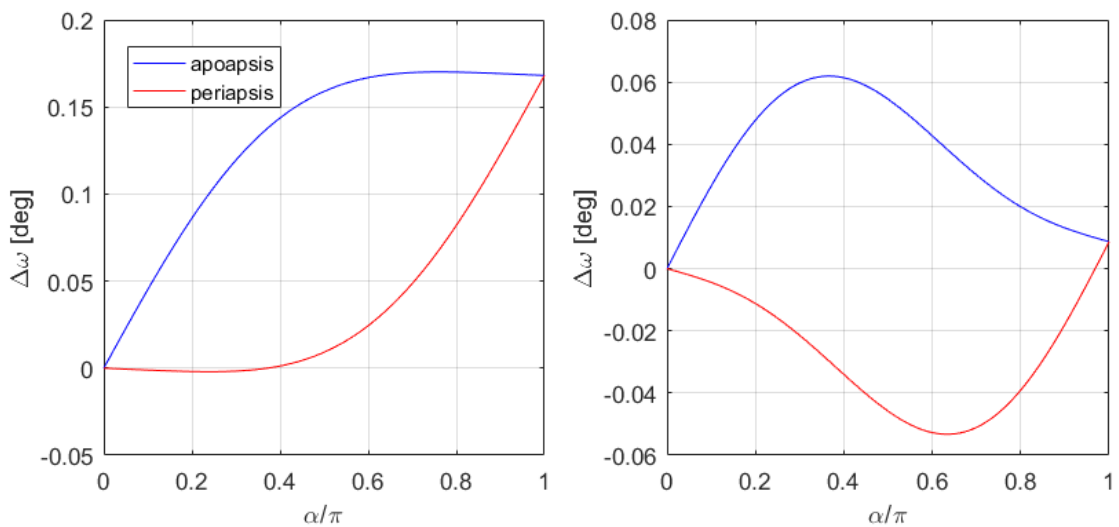


FIGURE 1.4: Rates of change in one revolution of a and e for cases (1), (2) and (3), in GTO orbit

of apoapsis or periapsis burns. We can observe that in steering law (2) we can modify a in a more efficient way compared to steering law (1), both in apogee and perigee burns. In steering law (3) the variation of a is not as effective, and with a continuous thrust ($\alpha = 180^\circ$) we can manage to modify e , keeping a constant.

In Fig. 1.5 it is shown the rate of change for i and Ω that is the same for all steering laws. In Fig. 1.6 we can notice the influence of the component f_{12} on steering law (4) for ω . In fact, the picture on the left represents the first three steering laws influenced only by f_3 , while in the right picture steering law (4) is shown.

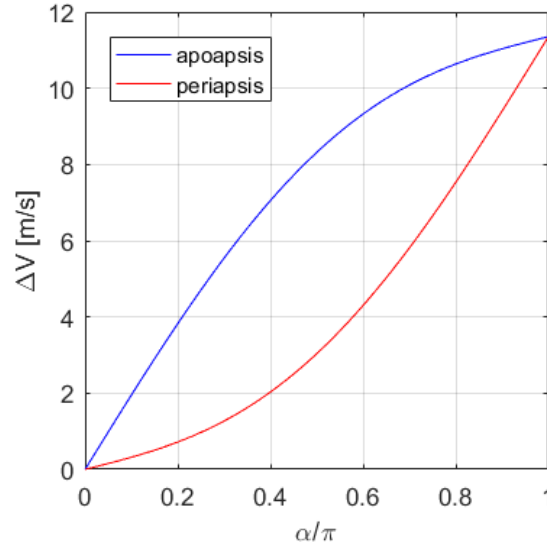
These results, especially the ones related to the out-of-plane component f_3 , vary greatly depending on initial data. In particular, a change in i is better performed with $\omega = 0^\circ, 180^\circ$

FIGURE 1.5: Rates of change in one revolution of i and Ω , in GTO orbitFIGURE 1.6: Rates of change in one revolution of ω , in GTO orbit [left: cases (1) (2) (3); right: case (4)]

and a change in Ω is better performed with $\omega = 90^\circ, 270^\circ$. Furthermore, apoapsis burns are more effective than periapsis burns in i , Ω and ω changes (with $\alpha < \pi/2$).

Finally, in Fig. 1.7 we can see the rate of change of ΔV , for apoapsis and periapsis burns.

Also for ΔV the results are the same for all steering laws.

FIGURE 1.7: Rate of change in one revolution of ΔV , in GTO orbit

1.3 Secular rates of change

Following Pollard's analysis, we can calculate the secular rates of change. In order to do this, we only have to divide the previous equations by the orbit period, obtaining the following results (complete operations are carried out in Appendix A).

1.3.1 Steering law (1)

$$\frac{da}{dt} = \frac{2f_{12}}{\pi} \sqrt{\frac{a^3}{\mu}(1-e^2)} \alpha \quad (1.22)$$

$$\frac{de}{dt} = -\frac{f_{12}}{2\pi} \sqrt{\frac{a}{\mu}(1-e^2)} (4\sigma \sin \alpha + 3e\alpha + e \sin \alpha \cos \alpha) \quad (1.23)$$

$$\frac{di}{dt} = -\frac{f_3}{2\pi} \sqrt{\frac{a}{\mu}} \cos \omega G(\sigma, \alpha, e) \quad (1.24)$$

$$\frac{d\Omega}{dt} = -\frac{f_3}{2\pi} \sqrt{\frac{a}{\mu}} \frac{\sin \omega}{\sin i} G(\sigma, \alpha, e) \quad (1.25)$$

$$\frac{d\omega}{dt} = \frac{f_3}{2\pi} \sqrt{\frac{a}{\mu}} \sin \omega \cot i G(\sigma, \alpha, e) \quad (1.26)$$

$$\frac{d\Delta V}{dt} = \frac{1}{\pi} \sqrt{(f_{12})^2 + (f_3)^2} (\alpha + \sigma e \sin \alpha) \quad (1.27)$$

1.3.2 Steering law (2)

$$\frac{da}{dt} = \frac{2f_{12}}{\pi} \sqrt{\frac{a^3}{\mu}} \int_0^\alpha \sqrt{1 - e^2 \cos^2 E} dE \quad (1.28)$$

$$\frac{de}{dt} = \frac{2f_{12}}{\pi} \sqrt{\frac{a}{\mu}} (1 - e^2) \int_0^\alpha \frac{\cos E (1 - e \cos E)}{\sqrt{1 - e^2 \cos^2 E}} dE \quad (1.29)$$

In case of apoapsis-centred burn, the limits of the integral are π and $\pi + \alpha$.

The expressions $\frac{di}{dt}$, $\frac{d\Omega}{dt}$, $\frac{d\omega}{dt}$, $\frac{d\Delta V}{dt}$ are the same as in case (1).

1.3.3 Steering law (3)

$$\frac{da}{dt} = -\frac{2\sigma f_{12}}{\pi} \sqrt{\frac{a^3}{\mu}} (1 - e^2) \sin \alpha \quad (1.30)$$

$$\frac{de}{dt} = \frac{f_{12}}{2\pi} \sqrt{\frac{a}{\mu}} (1 - e^2) (4\sigma e \sin \alpha + 3\alpha + \sin \alpha \cos \alpha) \quad (1.31)$$

The expressions $\frac{di}{dt}$, $\frac{d\Omega}{dt}$, $\frac{d\omega}{dt}$, $\frac{d\Delta V}{dt}$ are the same as in case (1).

1.3.4 Steering law (4)

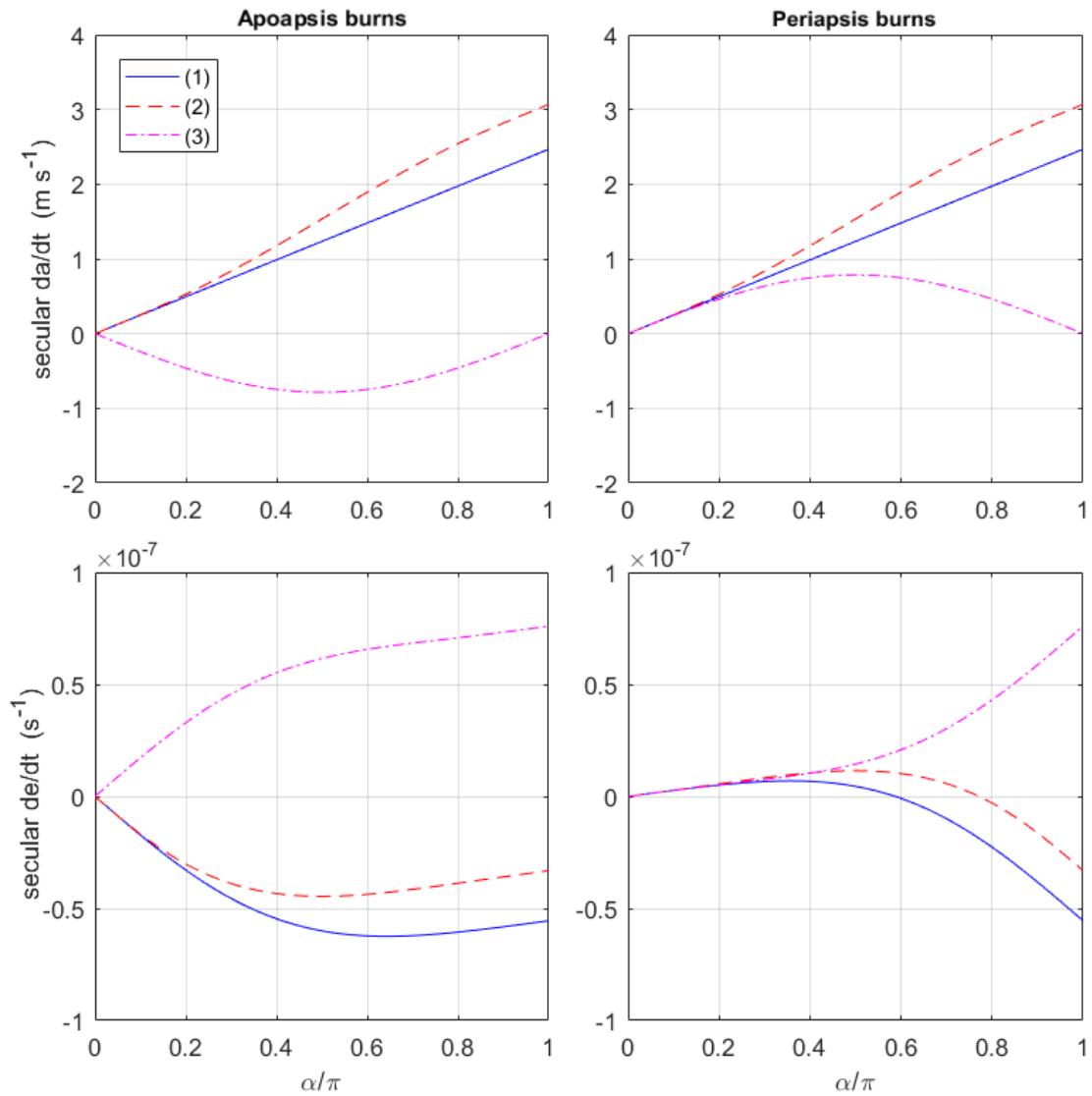
$$\frac{da}{dt} = 0 \quad (1.32)$$

$$\frac{de}{dt} = 0 \quad (1.33)$$

$$\frac{d\omega}{dt} = \frac{1}{2\pi} \sqrt{\frac{a}{\mu}} \left[f_{12} \frac{\sqrt{1 - e^2}}{e} (-2\sigma e \sin \alpha - 3\alpha + \sin \alpha \cos \alpha) + f_3 \sin \omega \cot i G(\sigma, \alpha, e) \right] \quad (1.34)$$

The expressions $\frac{di}{dt}$, $\frac{d\Omega}{dt}$, $\frac{d\Delta V}{dt}$ are the same as in case (1).

In Fig. 1.8 we can see the secular rates of a and e for the first three steering laws and for apoapsis or periapsis burns. For these graphs we have considered a typical GTO around the Earth (using μ_e) with $a = 24364$ km and $e = 0.7306$. As we can notice, they follow the same evolution of the rates of change. For our applications we will just use the rates of change in one revolution, as they are easier to understand and to control in our algorithm.

FIGURE 1.8: Secular rates of a and e for steering laws (1) (2) and (3), in Earth orbit

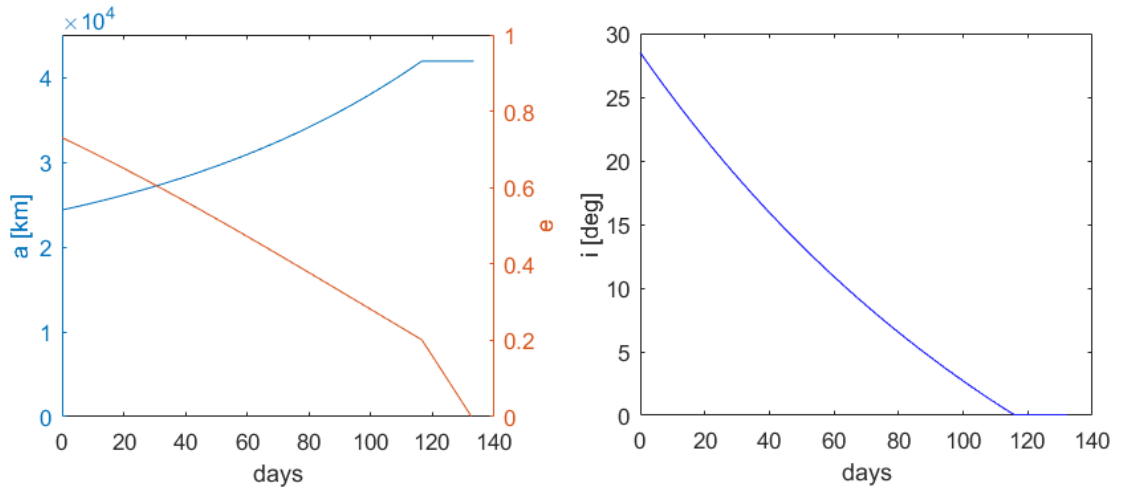
1.4 Application of GTO-to-GEO transfer

In order to validate the algorithms used in the next chapter, we analyse an application of a transfer from GTO to GEO, comparing the results of POLLARD97 for the same transfer. It is a transfer that involves all the orbital parameters, even if when we reach the GEO the values of e will be zero, and ω and Ω will not be defined. Therefore, the variation of these two parameters will not be important. The difference with Pollard's analysis is the use of the rates of change in one revolution instead of the secular rates of change.

The data of the initial and final orbit are listed in Table 1.2. Because of the closeness to Earth, we have to introduce the perturbation due to Earth's oblateness (J_2 factor) in equation 1.13 for the variation of ω . In fact, even if we do not care about the variation of ω , this value

TABLE 1.2: GTO-GEO data

	a [km]	e	i
GTO	24364	0.7306	28.5°
GEO	42164	0	0°

FIGURE 1.9: Evolution of a , e (left) and i (right) for a GTO-GEO transfer

appears in the equation 1.11 for the variation of i . In particular, the equation 1.13 becomes:

$$\Delta\omega = \frac{a^2}{\mu} f_3 \sin\omega \cot i G(\sigma, \alpha, e) + A(a, e, i) \quad (1.35)$$

where, with $J_2 = 0.00108263$ and the Earth's radius $R_e = 6738.137$ km:

$$A(a, e, i) = \frac{3\pi}{2} J_2 \left(\frac{R_e}{a} \right)^2 \frac{4 - 5 \sin^2 i}{(1 - e^2)^2} \quad (1.36)$$

As initial value of ω we take -15° , so that it approaches to zero when i reaches zero.

In according to Pollard, we take the yaw angle $\beta = 42.2^\circ$, in order to reach the desired values of a and i at the same time. For this part of the manoeuvre we use steering law (1), apogee centred burns and burn angle $\alpha = \pi/2$. At the end of this part we reach the desired values of a and i , and we only have to bring e to zero. It can be done with steering law (3) and a continuous in-plane burn ($\alpha = 180^\circ$). In fact, as we can remember from Fig. 1.4, this condition allows us to change e keeping the other orbital elements constant.

The evolution of the three orbital elements involved in the manoeuvre is reported in Fig. 1.9, using $\mu_e = 398601 \text{ km}^3/\text{s}^2$ and $f = 3 \cdot 10^{-7} \text{ km/s}^2$. Like POLLARD97, we obtain a total time of 133 days, and a total ΔV of 2.40 km/s. With other values of α for the first part of the manoeuvre, we can obtain other results with higher ΔV and lower total time or vice

versa.

With an impulsive burn the total ΔV would be 1.84 km/s. If we convert these two results in employed propellant mass, we can obtain that the propellant consumption for the impulsive burn is about 6 to 10 times more than the consumption with the low-thrust transfer. In conclusion, using a low-thrust transfer is convenient in term of employed propellant, but at the cost of a higher total manoeuvre time.

The formulation just presented is affected by singularities, because it is referred to the classical Lagrange planetary equations. In fact, we have singularities with i or e equal to zero, when Ω and ω are not defined. These cases will be discussed later, while in the next chapter we will see an application for a non-singular case, in particular a coplanar transfer with e and i different to zero.

Chapter 2

Jupiter's moons coplanar transfer

In this chapter we will present an application of Pollard's theory for a transfer between two moons of Jupiter (Europa and Ganymede). In particular, the method will be applied for a transfer between two coplanar orbits with $e \neq 0$. Thus, only the variation of a and e is studied. The objective of the method is to find how to better perform this manoeuvre, obtaining the ΔV and the total time of the optimal transfer.

This transfer is based on the work of Fantino and Castelli^[8] (2016), where the Jupiter's moons tour is performed using low energy transfers in combination with impulsive manoeuvres. Instead of these impulsive manoeuvres, using a low-thrust transfer can reduce the needed propellant.

2.1 Jupiter's moons tour

A possible and useful application of our method is related to the interplanetary manoeuvres employed in the Jovian system. The exploration of Jupiter's moons and, in particular, that of the four Galilean moons (Io, Europa, Ganymede, Callisto), is gaining increasingly higher scientific interest (Atkinson et al.^[12], 2009), because they may contain liquid water and they are good candidates for future human colonization. With this purpose, the past and future missions deal with the problem of the transfer between two moons or even of a tour among different moons. The simplest method for performing this tour is using impulsive burns, but it is also the most expensive in term of propellant. Gravity assists can help to reduce the amount of employed propellant, at the cost of higher transfer time.

TABLE 2.1: Jupiter's orbits data

	Initial orbit	Final orbit	Average orbit
a [km]	778054.59	900986.45	839522.02
e	0.118548	0.143747	0.1311475
μ_j [km ³ s ⁻²]	126654432.567		

Another method exploits the low-energy trajectories between the libration points of the three-body problems composed by Jupiter and each moon (Koon et al.^[13] 2001). The basic idea is to move along the stable and unstable invariant manifolds trajectories of two moons that have an intersection. Thus for example, the transfer from the outer to the inner moon starts from the point L_1 of the outer moon, it follows the unstable manifold until the intersection with the stable manifold of the inner moon, and it ends in the point L_2 of the inner moon. A simplification of this method is presented by Fantino and Castelli^[8] (2016) and it allows us to save computing time. It is based on dividing the transfer in two different parts: the first one when we are close to the moon and we apply the three-body problem; the second one when we are far enough away from the moon and we consider only the influence of Jupiter. It is considered a coplanar transfer, thus obtaining the trajectory from the planar Lyapunov orbits for the inner and outer moon respectively around L_2 and L_1 . These trajectories lead to different orbits defined by the orbital elements, looking for orbits with an intersection point that allows the transfer between the two orbits with an impulsive burn. This solution is viable for a single transfer between only two moons, but it would assume a too high cost if we want to perform a complete tour of the moons. Instead of the impulsive burn a low-thrust manoeuvre can be used, therefore we can apply the method developed in the previous chapter.

2.2 Europa-Ganymede coplanar transfer

We consider a transfer between Europa and Ganymede, disregarding Io for its high level of radiation, and we assume coplanar orbits thanks to the fact that the two moons have a little difference of inclination between each other. This hypothesis implies that we have to change only a and e , without considering i , ω and Ω , and as the fourth steering law does not affect a and e , it will not be considered. Data of the two orbits taken from Fantino and Castelli's analysis are listed in Tab. 2.1, and as we can see, we want to move from the inner

moon Europa to the outer moon Ganymede. The average orbit contains the average values between the initial and final orbits, and we will use these values in the next sections. μ_j is the gravitational parameter of Jupiter.

Our objective is to determine how to better perform this manoeuvre, calculating the ΔV and the total transfer time. First of all, we define the thrust mode as the combination of a steering law and a periapsis or apoapsis centred burns. In order to simplify control over the problem and the developed algorithm, we will use the rates of change equations in one revolution (1.9 to 1.18). For the solution of this problem, we have to pay attention to two different aspects that we will discuss: the first one concerns the hypothesis of a and e constant for several revolutions; the second one concerns the method of performing the transfer, for example applying determinate steering laws.

Regarding the first aspect, the equations just mentioned have been obtained assuming that the orbital parameters were constant during one revolution, and their formulation presents a and e as known values. Thus, applying them we can proceed in two different ways: we can update for each revolution the values of a and e knowing the variation of these two parameters, or we can keep a and e constants for all the revolutions. The second method is obviously less accurate, but it requires less computing time. In this analysis we want to calculate if the accuracy of the second method can be acceptable or not in respect to the first one. In order to reduce the error we will use the average values of the orbits instead of the initial values.

For the second aspect of the problem, we will study how to perform the transfer, firstly searching if it is possible to do the manoeuvre with the same steering law and with the same α . We will call the solution single thrust mode. Secondly searching if there are other options using different steering laws and different values of α . In particular, we will analyse the situation with two different modes of thrust, so it will be called double thrust mode.

Once we obtain the solution or the solutions, we will calculate the total ΔV and the total time of the manoeuvre, comparing the solutions in order to find the best one.

Finally, we will calculate the propellant mass for the best case, assuming realistic data of the thruster.

2.2.1 Jupiter secular rates of change

In order to make a comparison with the graphs of the Earth orbit obtained in the previous chapter (Fig. 1.8), we represent in Fig. 2.1 the equation of the secular rates of a and e for

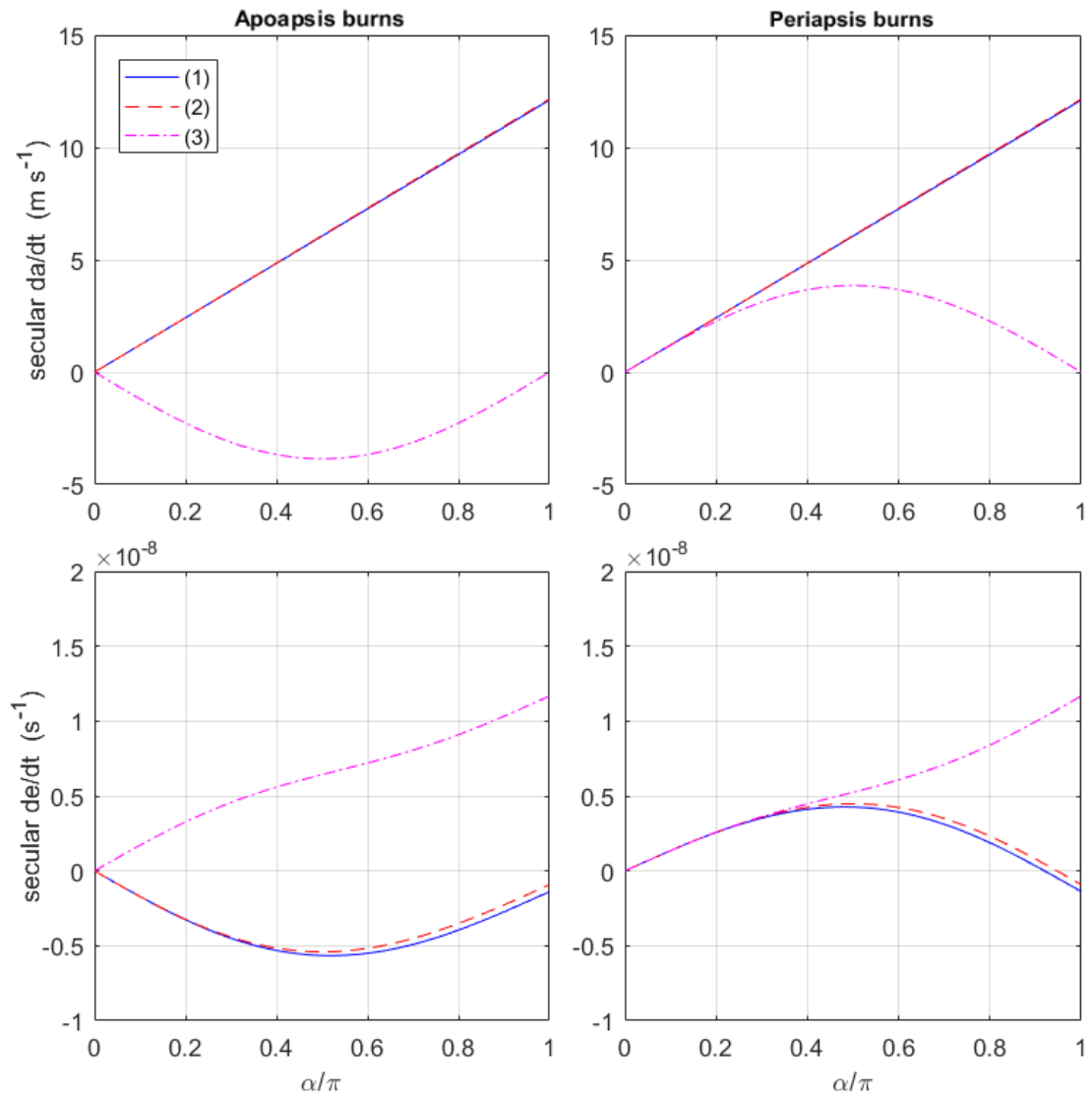


FIGURE 2.1: Secular rates of a and e for different cases, initial orbit around Jupiter

apoapsis and periapsis centred burns (1.22, 1.23, 1.28, 1.29, 1.30, 1.31) as functions of α/π , assuming that the orbital parameters do not change, so maintaining the values of the initial orbit. The first three steering laws are shown, because as the Earth orbits the fourth case does not affect a and e . The value of acceleration used now is $f_{12} = 1 \cdot 10^{-7} \text{ km/s}^2$, less compared to the Earth orbit because the electrical power of a spacecraft around Jupiter is less than the one around the Earth. Even if the evolution of the graphs is the same for both cases, we can notice that now the steering laws (1) and (2) give almost the same results because of the low eccentricity of the orbit.

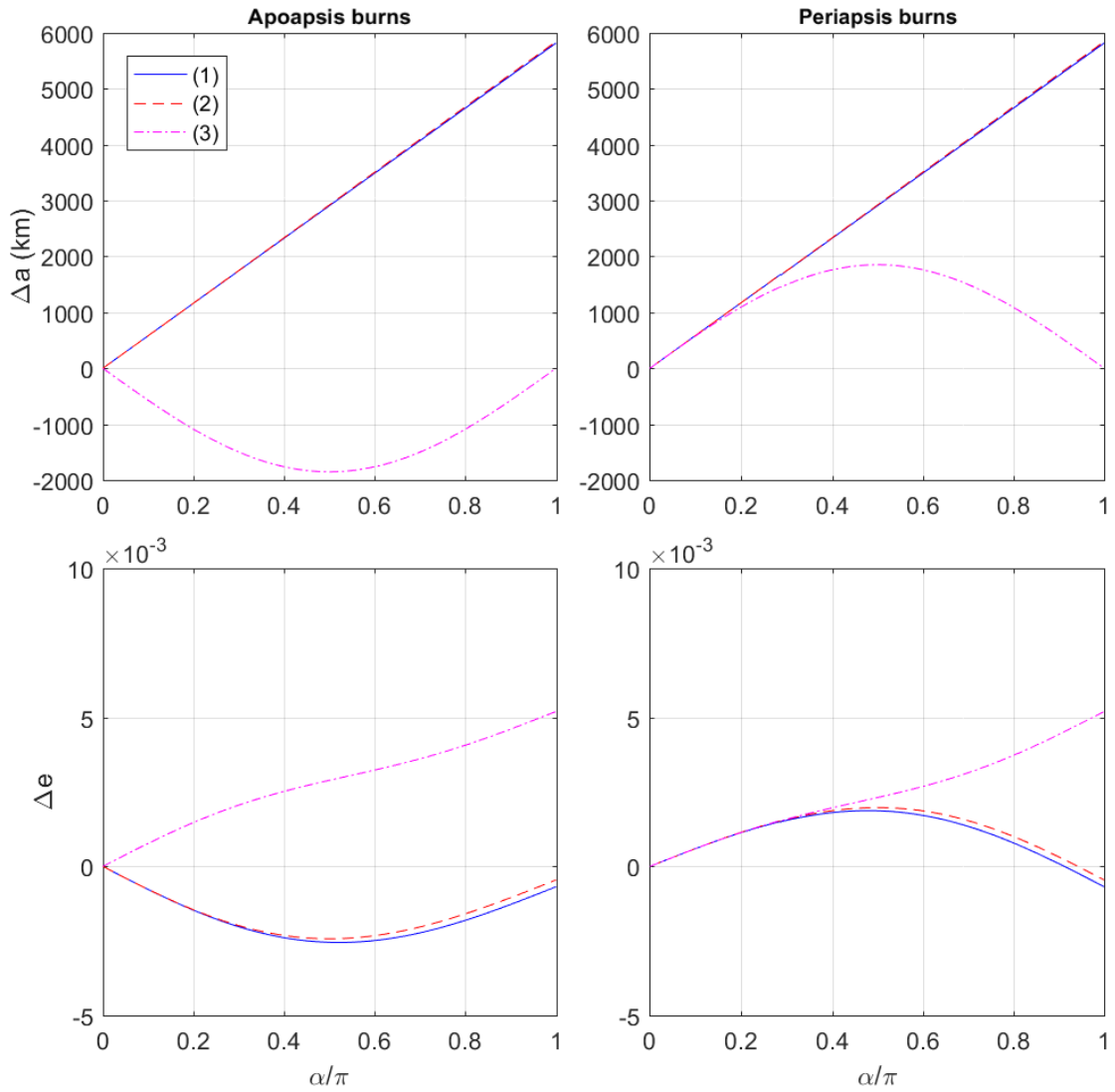


FIGURE 2.2: Rates of change of a and e in one revolution, average orbit around Jupiter

2.2.2 Jupiter rates of change in one revolution

A more appropriate graph could be that portrayed in Fig. 2.2, illustrating the variations of a and e in a single revolution, which are stated in the equations 1.9, 1.10, 1.15, 1.16, 1.17, 1.18. These graphs show how orbital parameters vary in a single revolution as functions of α/π and for the first three steering laws. The values of a and e used in the equations are the ones referred to the average orbit (Tab. 2.1). We will use these graphs, and consequently the related equations of the rates of change, because with them it is easier to search the number of revolutions needed to perform a required Δa_{req} or Δe_{req} , with a determinate α . In particular, after the selection of α and the steering law, we found in the graph the relative

Δa or Δe and as a first approximation the total number of revolutions n will be (for a):

$$n = \frac{\Delta a_{req}}{\Delta a} \quad (2.1)$$

2.3 Orbit transfer with single thrust mode

Knowing the rates of change, we want to find a way to perform the orbital transfer between the two orbits in a reasonable period of time and with a low ΔV . The total variations of the transfer for a and e are the following, using the values in Tab. 2.1:

$$\Delta a_{req} = a_{fin} - a_{in} = 122934.86 \text{ km} \quad (2.2)$$

$$\Delta e_{req} = e_{fin} - e_{in} = 0.025199 \quad (2.3)$$

2.3.1 Burn angle and number of revolutions for the single thrust mode

We want to study a simple case where we perform the manoeuvre with a single thrust mode, therefore with α constant and a single steering law during the entire manoeuvre. In order to do so, we want a and e to reach the desired value at the same time. For each steering law, and considering the periapsis or apoapsis burns, we calculate the number of revolutions that we need to obtain Δa_{req} and Δe_{req} as functions of α . To better explain this, Fig. 2.3 represents two examples of the graphs that can be obtained. Each point of the map gives the total variation Δa_{tot} or Δe_{tot} as functions of α and n . The black lines are isolines spaced of 10000 km for a (left graph) and 0.01 for e (right graph). The red line in the right graph is the isoline for $\Delta e_{tot} = 0$, while the magenta isoline represents the conditions necessary for α and n to achieve Δa_{req} and Δe_{req} . In order to reduce the error, these particular graphs are made using the average values of the orbits (Tab. 2.1) and for this reason they are accurate only near the magenta lines, where we really obtain those average values.

The magenta isolines are the ones that interest us, because if one of them exists it means that we are able to achieve the required variation in a fixed number of revolutions. Nevertheless, in order to perform the transfer with a single thrust mode, we have to obtain Δa_{req} and Δe_{req} at the same time. The solutions of this problem are given by the intersection points of the isolines of a and e for a determinate thrust mode. All these points will be the possible modes for performing the transfer in a single thrust mode, with a determinate α and in a

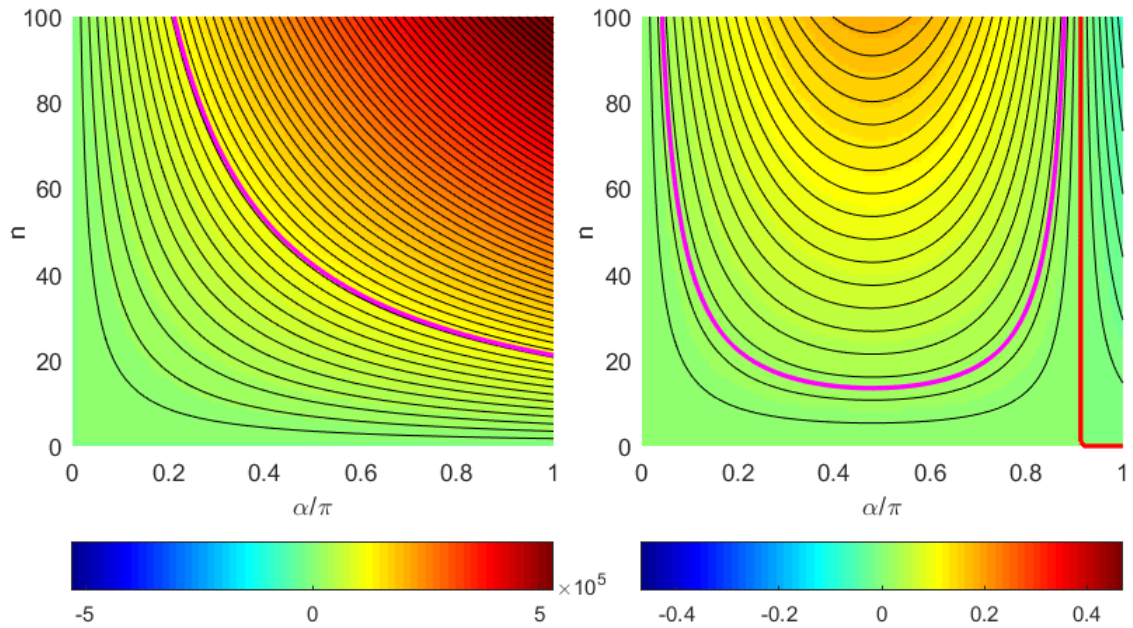


FIGURE 2.3: Δa_{tot} (left) and Δe_{tot} (right) as functions of burn arc and number of revolutions, periapsis burn, steering law (1)

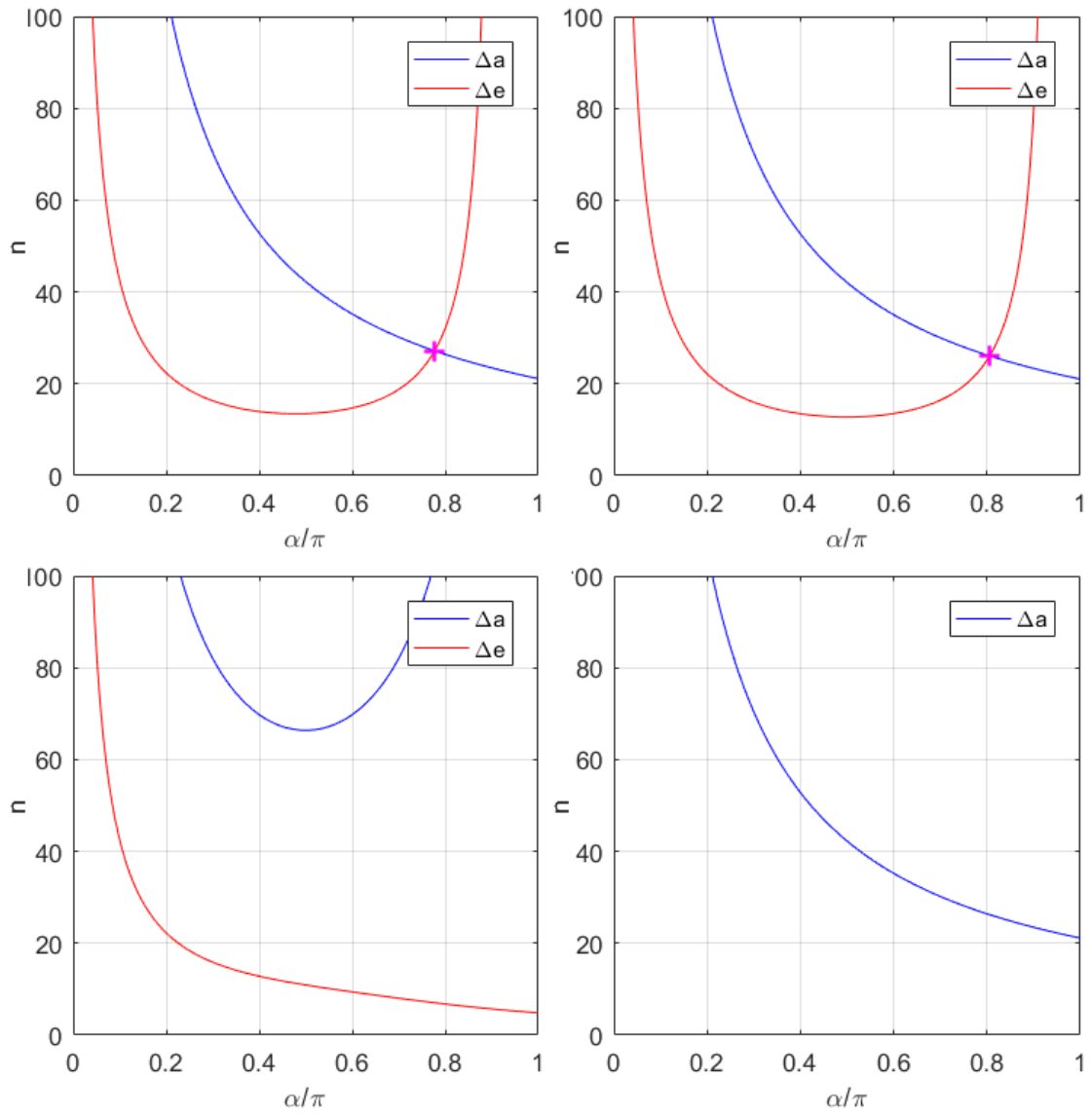
TABLE 2.2: Results of burn angle and number of revolutions for single thrust mode

Case	α/π	n
Case (1), periapsis	0.7772	27.1784
Case (2), periapsis	0.8057	26.0819

specific number of revolutions. In Fig. 2.4 we can appreciate the results for some cases. The upper graphs represent the two only cases with a solution. The coordinates of the intersection points are listed in Tab. 2.2, including the relative error between the two calculation methods. The lower graphs represent two cases without a possible solution.

2.3.2 Delta V and total time for the single thrust mode

As previously stated, the next step would be calculating the total ΔV and total time of the manoeuvre. As regards the first task, we use equation 1.14, while for the second one we calculate the orbital period and we multiply it for the number of revolutions. The solutions for the two cases found in the previous section are listed in 2.3.

FIGURE 2.4: Graphs of Δa_{req} and Δe_{req} for single thrust modeTABLE 2.3: Results of ΔV and total time for single thrust mode

Case	ΔV [m/s]	total time [days]
Case (1), periapsis	875.7529	135.0914
Case (2), periapsis	875.6735	129.6411

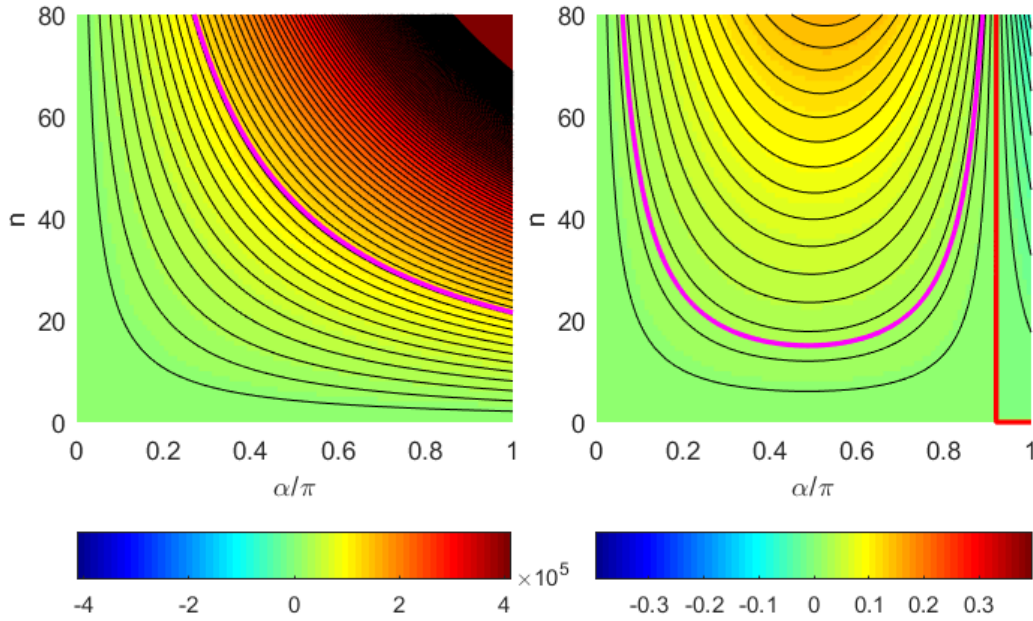


FIGURE 2.5: Δa_{tot} (left) and Δe_{tot} (right) as functions of burn arc and number of revolutions, periapsis burn, steering law (1)

2.4 Comparison of average and updated values

The results obtained assuming a and e constant during all the manoeuvres must be validated. In fact, although the total variations would not seem to be that significant, by using the values of the initial orbit or the values of the final orbit we can reach a difference of the Δa in a single revolution of 2560 km , and of 0.0015 for the Δe . With a large number of revolutions, these differences could be not acceptable.

A more accurate method consists on updating the values of a and e after each revolution, adding the terms Δa and Δe . Therefore, differently from before now these terms vary for each revolution just because of the variation of a and e . The algorithm is more complex, but the results are more precise as we can see in Fig. 2.5. The meaning of the isolines is the same described in section 2.3.1 for Fig. 2.3, but now we can see that with a high n and high α the total variation diverges because the orbits become much larger. In fact, here the results are accurate for every point of the graphs, and not only near the magenta lines.

Then, the process followed is the same of the previous section, looking for all the possible points of intersection for each thrust mode. The solutions of this method, together with a comparison and the relative error between the two methods is listed in Tab. 2.4.

In order to calculate ΔV and the total time of the manoeuvre, the process is slightly more complex. Now, for each revolution we have a different value of ΔV and period, thus we have to calculate them in each revolution, adding all together at the end. The solutions and

TABLE 2.4: Comparison results of burn angle and number of revolutions for single thrust mode

Case	Updated orbit	Average orbit	Relative error	
Case (1)	0.7779	0.7772	0.090 %	(α/π)
Periapsis	27.6624	27.1784	1.750 %	(n revolutions)
Case (2)	0.8064	0.8057	0.087 %	(α/π)
Periapsis	26.5568	26.0819	1.788 %	(n revolutions)

TABLE 2.5: Comparison results of ΔV and total time for single thrust mode

Case	Updated orbit	Average orbit	Relative error	
Case (1)	882.3645	875.7529	0.749 %	$(\Delta V \text{ [m/s]})$
Periapsis	135.9590	135.0914	0.638 %	(total time [days])
Case (2)	882.4398	875.6735	0.767 %	$(\Delta V \text{ [m/s]})$
Periapsis	130.4997	129.6411	0.658 %	(total time [days])

the comparison between the two calculation methods with the relative errors are presented in Tab. 2.5.

We can notice that the errors made using the approximation of constants a and e are enough small, and this allows us to use this hypothesis for the next operations.

2.5 Orbit transfer with double thrust mode

In the previous sections we found a possible solution for our problem, but that did not establish whether it referred to the minimum ΔV or the minimum total time of orbital transfer. For this reason, we will focus on the search for other possible solutions and then compare them. Differently from before, here we choose to analyse the transfer using two different thrust modes, remembering that with thrust mode we identify a combination of a steering law and periapsis or apoapsis centred burns. As demonstrated previously, we can use the values of the average orbit for a and e , keeping them constant for the entire manoeuvre. This hypothesis allows us to make an important simplification in the operations, as we are able to analytically resolve the following system of equations:

$$\begin{cases} n_1 \Delta a_{tot1} + n_2 \Delta a_{tot2} = \Delta a_{req} \\ n_1 \Delta e_{tot1} + n_2 \Delta e_{tot2} = \Delta e_{req} \end{cases} \quad (2.4)$$

where:

TABLE 2.6: Minimum ΔV and minimum total time for double thrust mode

Min ΔV [m/s]	874.1793
Total time [days]	198.4386
ΔV [m/s]	875.6736
Min total time [days]	129.6411

- n_1, n_2 are the numbers of revolutions for the first and the second thrust mode, unknowns of the system;
- $\Delta a_{tot1}, \Delta a_{tot2}, \Delta e_{tot1}, \Delta e_{tot2}$ are the variations of a and e for the first and the second thrust mode, functions only of α ;
- $\Delta a_{req}, \Delta e_{req}$ are the required variations of a and e (eq. 2.2, 2.3).

From which we obtain:

$$\begin{cases} n_2 = \frac{\Delta e_{req} \Delta a_{tot1} - \Delta a_{req} \Delta e_{tot1}}{\Delta a_{tot1} \Delta e_{tot2} - \Delta a_{tot2} \Delta e_{tot1}} \\ n_1 = \frac{\Delta a_{req} - n_2 \Delta a_{tot2}}{\Delta a_{tot1}} \end{cases} \quad (2.5)$$

It is important to point out the absence of the single thrust mode's solution, which would suppose the denominator of the equation of n_2 in Eq. 2.5 to be equal to zero.

We must notice that even α can present differences between the two cases. For each combination of two thrust modes and for each pair of burn angles, we calculate the two values of n , eliminating all the solutions with at least one of the $n < 0$, and all the solutions with an excessive number of revolutions, because the total time will be unacceptable. Therefore, we obtain 28 possible combinations of two thrust modes that allow us to perform the manoeuvre.

Knowing the number of revolutions and the burn angle used for each case, we can easily calculate the total ΔV and the total time of the manoeuvre. In Tab. 2.6 we can appreciate the results of the minimum ΔV and minimum total time, considering that all the solutions with the total number of revolutions higher than 40 (200 days) have been discarded. As we notice, the solution with the minimum ΔV is not preferable. In fact, it is only 1.5 m/s lower than the ΔV obtained with the single thrust mode (875.674 m/s), but it implies a significant increase in the number of days over the total time. The condition of minimum total time gives the same results as the single thrust mode, as it is obtained with both thrust modes in periapsis centred burns and in the steering law (2), and it also gives the same value of the burn angle ($\alpha/\pi = 0.806$).

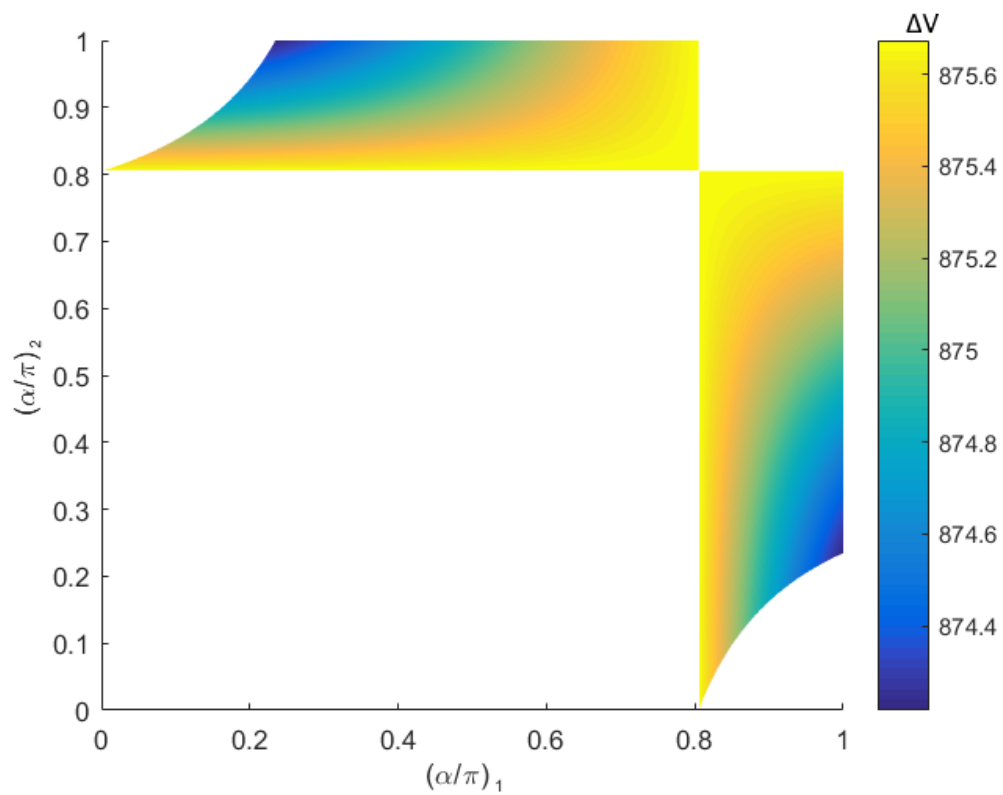
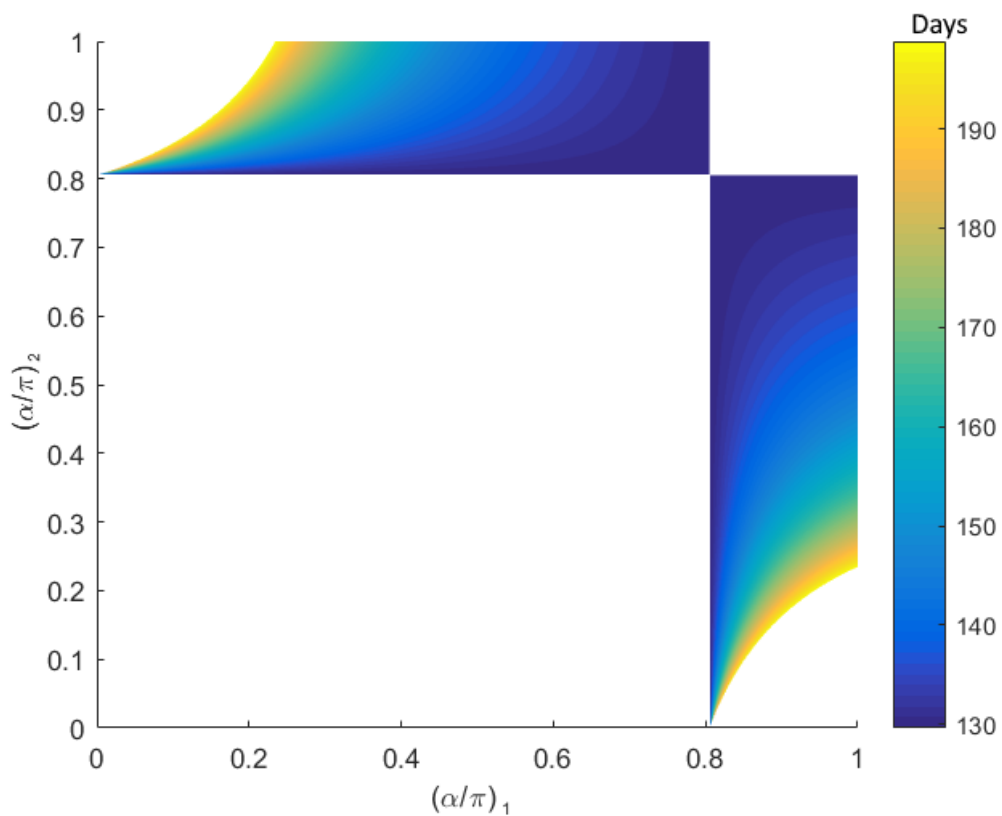
FIGURE 2.6: Total ΔV in function of burn angles for double thrust mode

FIGURE 2.7: Total time in function of burn angles for double thrust mode

In Fig. 2.6 and Fig. 2.7 the results are shown for the case with the minimum total time. The abscissa and ordinate hold a representation of the normalized burn angles of the first and second thrust mode respectively. We can notice that the variation of total ΔV is quite small between each point of the graphs, while the total time of the manoeuvre presents a larger variation. For this reason, the best solution could be the one with the minimum total time. We have to underline that the entire problem of finding the optimal solution is case dependent, therefore for each new problem we have to analyse the results and adopt the appropriate conclusion.

2.6 Propellant mass

In conclusion, we can assume that the result of the single thrust mode is acceptable, and it gives an easier method to find a quasi-optimal solution. For these results we can calculate the propellant mass required for our transfer. Assuming a dry mass of $m_f = 500$ kg and a specific impulse $I_{sc} = 3000$ s:

$$c = I_{sp} g_0 = 3000 \cdot 9.81 = 29430 \text{ m/s} \quad (2.6)$$

and using the Rocket equation (eq. 2.7) with $\Delta V = 882.44$ m/s (from Tab. 2.5), where $m_0 = m_f + m_p$ is the initial mass, m_p the propellant mass:

$$\frac{m_f}{m_0} = e^{-\frac{\Delta V}{c}} = 0.9705 \quad (2.7)$$

$$m_p = m_0 - m_f = 15.219 \text{ kg} \quad (2.8)$$

We obtain a propellant mass of 15.219 kg.

We can compare these results with the same transfer performed with an impulsive manoeuvre, obtained by Viale^[14] (2016). In that case, Viale obtained a ΔV of 881.4 m/s. Considering a chemical thruster with $I_{sc} = 400$ s and the same dry mass of the previous case, the propellant mass would be 125.9 kg, much bigger than the propellant mass for the low-thrust transfer.

Chapter 3

Singular case of inclination zero

The Lagrange planetary equations are affected by singularities when e or i are equals to zero. The case of $e = 0$ is an intrinsic singularity of the problem, but for our purpose it is not much interesting. In fact, it affects only a particular case: the orbital element ω with the steering law (4) when f_{12} is different to zero (see equation 1.21). Furthermore, ω is not defined when $e = 0$, thus its variation does not have great importance.

If $i = 0^\circ$, we have a singularity in equation 1.12 for the presence of $\sin i$ at the denominator, but also ω is not defined. For this reason, both equations 1.11 and 1.13 are not applicable, and we cannot obtain mathematically the variation of i when actually it could exist. In order to solve this problem, we have to analyse the nature of the orbital element i . i is not a geometrical element that characterizes the orbit, but it is an angular parameter that represents the position of the orbit compared to an external reference frame. If $i = 0^\circ$, the reference frame is not appropriate and we have to change it, for example applying a rotation around one of the axes. We will discuss a method to perform this rotation and an application in the case in which the longitude of the periapsis $\bar{\omega}$ is known.

3.1 From state vector to orbital elements

A possible solution is based on realizing a rotation around the unit vector \hat{I} of an angle φ (see Fig. 1.1 for the reference system). In order to do so, we can write the various factors as vectors, applying the operations for passing from the state vector to the orbital elements (Bate, Muller and White^[15], 1971).

- First of all, we transform the state vector with the rotation matrix. Therefore, we have to know the position and the velocity of a certain point of the orbit.

$$\vec{r}' = \begin{bmatrix} r'_X \\ r'_Y \\ r'_Z \end{bmatrix} = \begin{bmatrix} 1 & 0 & 0 \\ 0 & \cos \varphi & -\sin \varphi \\ 0 & \sin \varphi & \cos \varphi \end{bmatrix} \begin{bmatrix} r_X \\ r_Y \\ r_Z \end{bmatrix} \quad (3.1)$$

$$\vec{V}' = \begin{bmatrix} V'_X \\ V'_Y \\ V'_Z \end{bmatrix} = \begin{bmatrix} 1 & 0 & 0 \\ 0 & \cos \varphi & -\sin \varphi \\ 0 & \sin \varphi & \cos \varphi \end{bmatrix} \begin{bmatrix} V_X \\ V_Y \\ V_Z \end{bmatrix} \quad (3.2)$$

- The norm of the distance and the velocity will be:

$$r' = \sqrt{\vec{r}' \cdot \vec{r}'} \quad (3.3)$$

$$V' = \sqrt{\vec{V}' \cdot \vec{V}'} \quad (3.4)$$

- The radial velocity:

$$V'_r = \frac{\vec{r}' \cdot \vec{V}'}{r'} = (r'_X V'_X + r'_Y V'_Y + r'_Z V'_Z) / r' \quad (3.5)$$

- The specific angular momentum:

$$\vec{h}' = \vec{r}' \times \vec{V}' = \begin{vmatrix} \hat{I} & \hat{J} & \hat{K} \\ r'_X & r'_Y & r'_Z \\ V'_X & V'_Y & V'_Z \end{vmatrix} \quad (3.6)$$

The norm of which is:

$$h' = \sqrt{\vec{h}' \cdot \vec{h}'} \quad (3.7)$$

- The inclination:

$$i' = \cos^{-1} \left(\frac{h'_Z}{h'} \right) \quad (3.8)$$

It has to lie between 0° and 180° .

- The vector of the node line:

$$\vec{N}' = \hat{K} \times \vec{h}' = \begin{vmatrix} \hat{I} & \hat{J} & \hat{K} \\ 0 & 0 & 1 \\ h'_X & h'_Y & h'_Z \end{vmatrix} \quad (3.9)$$

The norm of which is:

$$N' = \sqrt{\vec{N}' \cdot \vec{N}'} \quad (3.10)$$

- The RAAN depends on the sign of N'_Y , so:

$$\Omega' = \begin{cases} \cos^{-1} \left(\frac{N'_X}{N'} \right) & \text{if } N'_Y \geq 0 \\ 360^\circ - \cos^{-1} \left(\frac{N'_X}{N'} \right) & \text{if } N'_Y < 0 \end{cases} \quad (3.11)$$

- The eccentricity vector:

$$\vec{e}' = \frac{1}{\mu} \left[\vec{V}' \times \vec{h}' - \mu \frac{\vec{r}'}{r'} \right] = \frac{1}{\mu} \left[\left(V'^2 - \frac{\mu}{r'} \right) \vec{r}' - r' V'_r \vec{V}' \right] \quad (3.12)$$

The norm of which is:

$$e' = \sqrt{\vec{e}' \cdot \vec{e}'} \quad (3.13)$$

- The argument of periaapsis depends on the sign of e'_Z , so:

$$\omega' = \begin{cases} \cos^{-1} \left(\frac{\vec{N}' \cdot \vec{e}'}{N' e'} \right) & \text{if } e'_Z \geq 0 \\ 360^\circ - \cos^{-1} \left(\frac{\vec{N}' \cdot \vec{e}'}{N' e'} \right) & \text{if } e'_Z < 0 \end{cases} \quad (3.14)$$

After all these operations, we obtain the orbital elements in the new reference frame. Together with a that does not change after the rotation, we are able to apply the equations of the rates of change as in the previous chapter.

3.2 From orbital elements to state vector

When the transfer is performed, we have to apply the opposite procedure to obtain the orbital elements in the initial reference system. In order to do this, we pass from the orbital elements to the state vector of any point of the orbit. The choice of this point does not affect the

result, so we will take the periapsis ($\nu = 0$). The equations used are the following:

$$\begin{cases} r'_x = r'(\cos \Omega' \cos \omega' - \sin \Omega' \cos i' \sin \omega') \\ r'_y = r'(\sin \Omega' \cos \omega' - \cos \Omega' \cos i' \sin \omega') \\ r'_z = r'(\sin i' \sin \omega') \end{cases} \quad (3.15)$$

$$\begin{cases} V'_x = -\sqrt{\frac{\mu}{a}} \sqrt{\frac{1+e'}{1-e'}} (\cos \Omega' \sin \omega' + \sin \Omega' \cos i' \cos \omega') \\ V'_y = -\sqrt{\frac{\mu}{a}} \sqrt{\frac{1+e'}{1-e'}} (\sin \Omega' \sin \omega' + \cos \Omega' \cos i' \cos \omega') \\ V'_z = -\sqrt{\frac{\mu}{a}} \sqrt{\frac{1+e'}{1-e'}} \sin i' \cos \omega' \end{cases} \quad (3.16)$$

In order to obtain the state vector in the initial reference frame, we have to apply the inverse rotation matrix to the state vector.

$$\vec{r} = \begin{bmatrix} r_X \\ r_Y \\ r_Z \end{bmatrix} = \begin{bmatrix} 1 & 0 & 0 \\ 0 & \cos \varphi & \sin \varphi \\ 0 & -\sin \varphi & \cos \varphi \end{bmatrix} \begin{bmatrix} r'_X \\ r'_Y \\ r'_Z \end{bmatrix} \quad (3.17)$$

$$\vec{V} = \begin{bmatrix} V_X \\ V_Y \\ V_Z \end{bmatrix} = \begin{bmatrix} 1 & 0 & 0 \\ 0 & \cos \varphi & \sin \varphi \\ 0 & -\sin \varphi & \cos \varphi \end{bmatrix} \begin{bmatrix} V'_X \\ V'_Y \\ V'_Z \end{bmatrix} \quad (3.18)$$

Finally, using again equations 3.3 to 3.14 we obtain the orbital elements expressed in the original reference frame after the manoeuvre.

3.3 Application of inclination = 0

Taking into account an orbit with $i = 0^\circ$, a way to calculate the state vector is knowing the longitude of the periapsis $\bar{\omega}$ (we remember that $\bar{\omega} = \omega + \Omega$), which is fixed also in case of $i = 0$ (see Fig. 3.1). In fact, we can write the position and velocity as:

$$\vec{r} = r \cos \bar{\omega} \hat{I} + r \sin \bar{\omega} \hat{J} + 0 \hat{K} \quad (3.19)$$

$$\vec{V} = -V \sin \bar{\omega} \hat{I} + V \cos \bar{\omega} \hat{J} + 0 \hat{K} \quad (3.20)$$

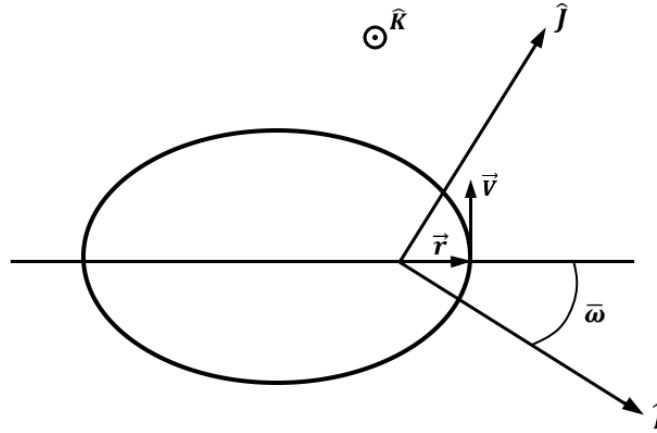
FIGURE 3.1: Reference system for an orbit with $i = 0$

TABLE 3.1: Orbit data after the rotation

e'	i'	ω'	Ω'
0.7306	30°	15°	0°

Where r is the module of the distance to the periastris, and V is the module of the velocity in the periastris and it can be obtained as:

$$V = \sqrt{\mu \left(\frac{2}{r} - \frac{1}{a} \right)} \quad (3.21)$$

Applying the equations of the previous sections for an Earth orbit with $r = 6563$ km, $a = 24364$ km, $\bar{\omega} = 15^\circ$ and $\varphi = 30^\circ$ we obtain the results listed in Tab. 3.1. A proof that the results are correct is given by Ω . In fact, it has to be 0° because the rotation is done around the unit vector \hat{I} and the node line will be along that direction. Another proof is given by the value of e that does not have to change after the rotation.

Finally, we notice that using $\bar{\omega}$ to find the state vector, the solution is simple: $i' = \varphi$ and $\omega' = \bar{\omega}$.

Conclusion

The exploration of the solar system is a topical issue for space missions, including the exploration of Jupiter's moons. Nowadays, there are many mission proposals to make this tour possible using viable methods of transfer and interesting trajectories. One of the purposes of this thesis was to find a way to perform the Jupiter's moons tour, benefiting from low-thrust transfers. The starting point was the analysis of low-thrust transfers using simplified steering laws, based on the work of Pollard^[9]. This method allows to geometrically control the entire problem, knowing the variation of the Keplerian orbital elements for each revolution. In addition, we know that these steering laws give a quasi-optimal result, as they are the optimal solution for easier cases. Furthermore, it is a more feasible method in the integration within a spacecraft, thanks to the simplicity of the steering laws. We have validated the algorithms used to calculate the variation of the orbital elements, comparing the case of GTO-to-GEO transfer with Pollard results. After validating the algorithms, we have analysed the Jupiter's moons tour. The low-thrust transfer is part of the work of Fantino and Castelli^[8], based on a low energy transfer in case of coplanar orbits. The entire transfer can be divided into two parts: the first one employing the invariant manifolds when the spacecraft is near to one of the moons (three-body problem); the second one that uses the low-thrust transfer to move between two coplanar and Keplerian orbits (two-body problem). This second part was solved using the method and the previously developed algorithms, in particular for the coplanar transfer between Europa and Ganymede. The purpose of these algorithms was to find the best steering case and burn angle, and to calculate the ΔV and the total time of the transfer. In order to validate the hypothesis and the results, we have studied different cases. First, we have seen that using the average values between the initial and final orbit gives an acceptable error compared to updating these values after each revolution (relative error lower than 0.8%). The total ΔV obtained for the best transfer is 882.4 m/s and the total time of the transfer is 130.5 days. Furthermore, we have analysed the same transfer

using a combination of steering laws. In order to solve the system of equations, we studied the transfer using two distinct steering cases and two distinct burn angles. We obtained that, for this specific problem, the best transfer is the same as we had using a single steering law. However, for a general case, thanks to this method, we are able to obtain different results of ΔV and total time of transfer. The limitation of this method is that if we want to use three distinct steering laws we have to resolve an underdetermined system of three equations. Future developments could take into account this problem. Another interesting development could be considering the 3D version of the moons' transfer. Instead of the Lyapunov orbits, it is based on the Halo orbits of two Galilean moons (Fantino et al.^[16], 2018). Therefore, the low-thrust transfer has to consider a 3D manoeuvre that affects all the orbital elements. The other important result obtained in this thesis deals with the singularity that affects the Lagrange planetary equations. In particular, we found a method that allows us to use these equations even when the inclination is equal to zero. This method is based on the properties of inclination that depend on the reference frame used. We applied an appropriate rotation of the reference frame around the axis \hat{I} , and used the operations needed to pass from the state vector to the orbital elements. With these operations we were able to find the orbital elements after the rotation. The method is highly efficient and if the longitude of the periapsis is known, the result after the rotation is immediate: $i' = \varphi$ and $\omega' = \bar{\omega}$.

A possible future work could deal with the singularity of eccentricity equal to zero. Nevertheless, this singularity does not particularly affect our model since when $e = 0$ the argument of periapsis is not defined. For this reason, we can assume that the periapsis or the apoapsis is in the most appropriate point of the orbit, in order to obtain the variation of the orbital elements that we want to achieve. In other words, we can apply the thrust considering the centre of the burn arc where it is more convenient.

In conclusion, in this thesis we have achieved two important objectives. We have developed an algorithm that deals with orbital transfers using one or two simplified steering laws, applying it to the exploration of Jupiter's moons, and we have solved the problem of Lagrange planetary equations singularity with inclination equal to zero. These results are presented here in an innovative and original way, being of great interest for the scientific community.

Appendix A

Operations for secular rates equations

Solving these calculations we have to remember that the integrals are centred with $\alpha = 0$ at the periapsis or $\alpha = \pi$ at the apoapsis. For this reason the odd functions and the functions with a rotational symmetry with respect to the point $\alpha = \pi$, like ' $\sin \alpha$ ' or ' $\cos \alpha \sin \alpha$ ', give no contribution to the integral.

A.1 Case 1

For the first case, with the in-plane accelerations perpendicular to the orbit path, we have $f_1 = 0$ and $f_2 = f_{12}$.

A.1.1 Semi-major axis $\frac{da}{dE}$

Starting from Eq. 1.2:

$$\frac{da}{dE} = \frac{2a^3}{\mu} \left(f_1 e \sin E + f_2 \sqrt{1 - e^2} \right)$$

with steering case 1, we obtain:

$$\frac{da}{dE} = \frac{2a^3}{\mu} f_{12} \sqrt{1 - e^2}$$

$$\Delta a = \int_{-\alpha}^{\alpha} \left(\frac{2a^3}{\mu} f_{12} \sqrt{1 - e^2} \right) dE$$

$$\Delta a = \frac{4a^3}{\mu} f_{12} \sqrt{1-e^2} \alpha$$

In order to obtain the secular rates of change we have to divide by the orbit period:

$$\frac{da}{dt} = \frac{1}{2\pi} \sqrt{\frac{\mu}{a^3}} \left(\frac{4a^3}{\mu} f_{12} \sqrt{1-e^2} \right) \alpha$$

$$\frac{da}{dt} = \frac{2f_{12}}{\pi} \sqrt{\frac{a^3}{\mu}} (1-e^2) \alpha$$

In case of apoapsis-centred burn, the limits of the integral are $\pi - \alpha$ and $\pi + \alpha$, and we obtain the same result.

A.1.2 Eccentricity $\frac{de}{dE}$

Starting from Eq. 1.3:

$$\frac{de}{dE} = \frac{a^2}{\mu} \left[f_1(1-e^2) \sin E + f_2 \sqrt{1-e^2} (2 \cos E - e - e \cos^2 E) \right]$$

with steering case 1, we obtain:

$$\frac{de}{dE} = \frac{a^2}{\mu} f_{12} \sqrt{1-e^2} (2 \cos E - e - e \cos^2 E)$$

$$\Delta e = \int_{-\alpha}^{\alpha} \left(\frac{a^2}{\mu} f_{12} \sqrt{1-e^2} (2 \cos E - e - e \cos^2 E) \right) dE$$

$$\Delta e = \frac{a^2}{\mu} f_{12} \sqrt{1-e^2} \left(4 \sin \alpha - 2e\alpha - \frac{e}{2} (2\alpha + 2 \sin \alpha \cos \alpha) \right)$$

In order to obtain the secular rates of change we have to divide by the orbit period:

$$\frac{de}{dt} = \frac{1}{2\pi} \sqrt{\frac{\mu}{a^3}} \frac{a^2}{\mu} f_{12} \sqrt{1-e^2} (4 \sin \alpha - 3e\alpha - e \sin \alpha \cos \alpha)$$

$$\frac{de}{dt} = \frac{f_{12}}{2\pi} \sqrt{\frac{a}{\mu}} (1-e^2) (4 \sin \alpha - 3e\alpha - e \sin \alpha \cos \alpha)$$

In case of apoapsis-centred burn, the limits of the integral are $\pi - \alpha$ and $\pi + \alpha$, and we obtain:

$$\frac{de}{dt} = \frac{f_{12}}{2\pi} \sqrt{\frac{a}{\mu}} (1-e^2) (-4 \sin \alpha - 3e\alpha - e \sin \alpha \cos \alpha)$$

A.1.3 Inclination $\frac{di}{dE}$

Starting from Eq. 1.4:

$$\frac{di}{dE} = \frac{a^2}{\mu} f_3 (1 - e \cos E) \left[\frac{(\cos E - e) \cos \omega}{\sqrt{1 - e^2}} - \sin E \sin \omega \right]$$

we obtain with all the steering cases (because it is not function of f_1 or f_2):

$$\begin{aligned} \Delta i &= \int_{-\alpha}^{\alpha} \left(\frac{a^2}{\mu} f_3 (1 - e \cos E) \left[\frac{(\cos E - e) \cos \omega}{\sqrt{1 - e^2}} - \sin E \sin \omega \right] \right) dE \\ \Delta i &= \frac{a^2}{\mu} f_3 \left[\frac{2(\sin \alpha - e\alpha) \cos \omega}{\sqrt{1 - e^2}} - \frac{e(\alpha + \sin \alpha \cos \alpha) \cos \omega}{\sqrt{1 - e^2}} + \frac{2e^2 \sin \alpha \cos \omega}{\sqrt{1 - e^2}} \right] \end{aligned}$$

In order to obtain the secular rates of change we have to divide by the orbit period:

$$\begin{aligned} \frac{di}{dt} &= \frac{1}{2\pi} \sqrt{\frac{\mu}{a^3}} \frac{a^2}{\mu} \frac{\cos \omega}{\sqrt{1 - e^2}} f_3 [2(\sin \alpha - e\alpha) - e(\alpha + \sin \alpha \cos \alpha) + 2e^2 \sin \alpha] \\ \frac{di}{dt} &= \frac{f_3}{2\pi} \sqrt{\frac{a}{\mu}} \frac{\cos \omega}{\sqrt{1 - e^2}} [2 \sin \alpha (1 + e^2) - 3e\alpha - e \sin \alpha \cos \alpha] \end{aligned}$$

In case of apoapsis-centred burn, the limits of the integral are $\pi - \alpha$ and $\pi + \alpha$, and we obtain:

$$\frac{di}{dt} = \frac{f_3}{2\pi} \sqrt{\frac{a}{\mu}} \frac{\cos \omega}{\sqrt{1 - e^2}} [-2 \sin \alpha (1 + e^2) - 3e\alpha - e \sin \alpha \cos \alpha]$$

A.1.4 RAAN $\frac{d\Omega}{dE}$

Starting from Eq. 1.5:

$$\frac{d\Omega}{dE} = \frac{a^2}{\mu} f_3 \frac{(1 - e \cos E)}{\sin i} \left[\frac{(\cos E - e) \sin \omega}{\sqrt{1 - e^2}} + \sin E \cos \omega \right]$$

we obtain with all the steering cases (because it is not function of f_1 or f_2):

$$\begin{aligned} \Delta \Omega &= \int_{-\alpha}^{\alpha} \left(\frac{a^2}{\mu} f_3 \frac{(1 - e \cos E)}{\sin i} \left[\frac{(\cos E - e) \sin \omega}{\sqrt{1 - e^2}} + \sin E \cos \omega \right] \right) dE \\ \Delta \Omega &= \frac{a^2}{\mu} f_3 \frac{1}{\sin i} \left[\frac{2(\sin \alpha - e\alpha) \sin \omega}{\sqrt{1 - e^2}} - \frac{e(\alpha + \sin \alpha \cos \alpha) \sin \omega}{\sqrt{1 - e^2}} + \frac{2e^2 \sin \alpha \sin \omega}{\sqrt{1 - e^2}} \right] \end{aligned}$$

In order to obtain the secular rates of change we have to divide by the orbit period:

$$\frac{d\Omega}{dt} = \frac{1}{2\pi} \sqrt{\frac{\mu}{a^3}} \frac{a^2}{\mu} \frac{\sin \omega}{\sin i} \frac{1}{\sqrt{1-e^2}} f_3 [2(\sin \alpha - e\alpha) - e(\alpha + \sin \alpha \cos \alpha) + 2e^2 \sin \alpha]$$

$$\frac{d\Omega}{dt} = \frac{f_3}{2\pi} \sqrt{\frac{a}{\mu}} \frac{\sin \omega}{\sin i} \frac{1}{\sqrt{1-e^2}} [2 \sin \alpha (1 + e^2) - 3e\alpha - e \sin \alpha \cos \alpha]$$

In case of apoapsis-centred burn, the limits of the integral are $\pi - \alpha$ and $\pi + \alpha$, and we obtain:

$$\frac{d\Omega}{dt} = \frac{f_3}{2\pi} \sqrt{\frac{a}{\mu}} \frac{\sin \omega}{\sin i} \frac{1}{\sqrt{1-e^2}} [-2 \sin \alpha (1 + e^2) - 3e\alpha - e \sin \alpha \cos \alpha]$$

A.1.5 Argument of periapsis $\frac{d\omega}{dE}$

Starting from Eq. 1.6:

$$\begin{aligned} \frac{d\omega}{dE} = \frac{a^2}{\mu} \left\{ \frac{1}{e} \left[-f_1 \sqrt{1-e^2} (\cos E - e) + f_2 (2 - e^2 - e \cos E) \sin E \right] - \right. \\ \left. - f_3 (1 - e \cos E) \cot i \left[\frac{(\cos E - e) \sin \omega}{\sqrt{1-e^2}} + \sin E \cos \omega \right] \right\} \end{aligned}$$

with steering case 1, we obtain:

$$\frac{d\omega}{dE} = \frac{a^2}{\mu} \left\{ \frac{f_{12}}{e} (2 - e^2 - e \cos E) \sin E - f_3 (1 - e \cos E) \cot i \left[\frac{(\cos E - e) \sin \omega}{\sqrt{1-e^2}} + \sin E \cos \omega \right] \right\}$$

$$\begin{aligned} \Delta\omega = \int_{-\alpha}^{\alpha} \left(\frac{a^2}{\mu} \left\{ \frac{f_{12}}{e} (2 - e^2 - e \cos E) \sin E - \right. \right. \\ \left. \left. - f_3 (1 - e \cos E) \cot i \left[\frac{(\cos E - e) \sin \omega}{\sqrt{1-e^2}} + \sin E \cos \omega \right] \right\} \right) dE \end{aligned}$$

$$\Delta\omega = -\frac{a^2}{\mu} f_3 \cot i \left[\frac{2(\sin \alpha - e\alpha) \sin \omega}{\sqrt{1-e^2}} - \frac{e(\alpha + \sin \alpha \cos \alpha) \sin \omega}{\sqrt{1-e^2}} + \frac{2e^2 \sin \alpha \sin \omega}{\sqrt{1-e^2}} \right]$$

In order to obtain the secular rates of change we have to divide by the orbit period:

$$\frac{d\omega}{dt} = -\frac{1}{2\pi} \sqrt{\frac{\mu}{a^3}} \frac{a^2}{\mu} \frac{\sin \omega}{\sqrt{1-e^2}} f_3 \cot i [2(\sin \alpha - e\alpha) - e(\alpha + \sin \alpha \cos \alpha) + 2e^2 \sin \alpha]$$

$$\frac{d\omega}{dt} = -\frac{f_3}{2\pi} \sqrt{\frac{a}{\mu}} \frac{\sin \omega}{\sqrt{1-e^2}} \cot i [2 \sin \alpha (1 + e^2) - 3e\alpha - e \sin \alpha \cos \alpha]$$

In case of apoapsis-centred burn, the limits of the integral are $\pi - \alpha$ and $\pi + \alpha$, and we obtain:

$$\frac{d\omega}{dt} = -\frac{f_3}{2\pi} \sqrt{\frac{a}{\mu}} \frac{\sin \omega}{\sqrt{1-e^2}} \cot i [-2 \sin \alpha (1+e^2) - 3e\alpha - e \sin \alpha \cos \alpha]$$

A.2 Case 2

For the second case, with the in-plane accelerations tangent to the orbit path, we have

$$f_1 = \frac{f_{12} e \sin E}{\sqrt{1-e^2 \cos^2 E}} \text{ and } f_2 = f_{12} \sqrt{\frac{1-e^2}{1-e^2 \cos^2 E}}.$$

A.2.1 Semi-major axis $\frac{da}{dE}$

Starting from Eq. 1.2:

$$\frac{da}{dE} = \frac{2a^3}{\mu} \left(f_1 e \sin E + f_2 \sqrt{1-e^2} \right)$$

with steering case 2, we obtain:

$$\frac{da}{dE} = \frac{2a^3}{\mu} \left(\frac{f_{12} e \sin E}{\sqrt{1-e^2 \cos^2 E}} e \sin E + f_{12} \sqrt{\frac{1-e^2}{1-e^2 \cos^2 E}} \sqrt{1-e^2} \right)$$

$$\Delta a = \int_{-\alpha}^{\alpha} \left[\frac{2a^3}{\mu} f_{12} \left(\frac{e^2 - e^2 \cos^2 E + 1 - e^2}{\sqrt{1-e^2 \cos^2 E}} \right) \right] dE$$

$$\Delta a = \frac{2a^3}{\mu} f_{12} \int_{-\alpha}^{\alpha} \sqrt{1-e^2 \cos^2 E} dE$$

In order to obtain the secular rates of change we have to divide by the orbit period:

$$\frac{da}{dt} = \frac{1}{2\pi} \sqrt{\frac{\mu}{a^3}} \frac{2a^3}{\mu} f_{12} \int_{-\alpha}^{\alpha} \sqrt{1-e^2 \cos^2 E} dE$$

$$\frac{da}{dt} = \frac{f_{12}}{\pi} \sqrt{\frac{a^3}{\mu}} \int_{-\alpha}^{\alpha} \sqrt{1-e^2 \cos^2 E} dE$$

In case of apoapsis-centred burn, the limits of the integral are $\pi - \alpha$ and $\pi + \alpha$, and we obtain the same result.

A.2.2 Eccentricity $\frac{de}{dE}$

Starting from Eq. 1.3:

$$\frac{de}{dE} = \frac{a^2}{\mu} \left[f_1(1 - e^2) \sin E + f_2 \sqrt{1 - e^2} (2 \cos E - e - e \cos^2 E) \right]$$

with steering case 2, we obtain:

$$\frac{de}{dE} = \frac{a^2}{\mu} \left[\frac{f_{12} e \sin E}{\sqrt{1 - e^2 \cos^2 E}} (1 - e^2) \sin E + f_{12} \sqrt{\frac{1 - e^2}{1 - e^2 \cos^2 E}} \sqrt{1 - e^2} (2 \cos E - e - e \cos^2 E) \right]$$

$$\Delta e = \int_{-\alpha}^{\alpha} \left[\frac{a^2}{\mu} f_{12} (1 - e^2) \left(\frac{e \sin^2 E + 2 \cos E - e - e \cos^2 E}{\sqrt{1 - e^2 \cos^2 E}} \right) \right] dE$$

$$\Delta e = \frac{a^2}{\mu} f_{12} (1 - e^2) \int_{-\alpha}^{\alpha} \frac{2 \cos E - 2e \cos^2 E}{\sqrt{1 - e^2 \cos^2 E}} dE$$

In order to obtain the secular rates of change we have to divide by the orbit period:

$$\frac{de}{dt} = \frac{1}{2\pi} \sqrt{\frac{\mu}{a^3}} \frac{a^2}{\mu} f_{12} (1 - e^2) 2 \int_{-\alpha}^{\alpha} \frac{\cos E (1 - e \cos E)}{\sqrt{1 - e^2 \cos^2 E}} dE$$

$$\frac{de}{dt} = \frac{f_{12}}{\pi} \sqrt{\frac{a}{\mu}} (1 - e^2) \int_{-\alpha}^{\alpha} \frac{\cos E (1 - e \cos E)}{\sqrt{1 - e^2 \cos^2 E}} dE$$

In case of apoapsis-centred burn, the limits of the integral are $\pi - \alpha$ and $\pi + \alpha$.

A.2.3 Inclination $\frac{di}{dE}$

We reach the same result as in case 1 because it is not function of f_1 or f_2 . See A.1.3.

A.2.4 RAAN $\frac{d\Omega}{dE}$

We reach the same result as in case 1 because it is not function of f_1 or f_2 . See A.1.4.

A.2.5 Argument of periapsis $\frac{d\omega}{dE}$

Starting from Eq. 1.6:

$$\frac{d\omega}{dE} = \frac{a^2}{\mu} \left\{ \frac{1}{e} \left[-f_1 \sqrt{1-e^2} (\cos E - e) + f_2 (2 - e^2 - e \cos E) \sin E \right] - f_3 (1 - e \cos E) \cot i \left[\frac{(\cos E - e) \sin \omega}{\sqrt{1-e^2}} + \sin E \cos \omega \right] \right\}$$

with steering case 2, we obtain:

$$\begin{aligned} \frac{d\omega}{dE} &= \frac{a^2}{\mu} \left\{ \frac{1}{e} \left[-\frac{f_{12} e \sin E}{\sqrt{1-e^2 \cos^2 E}} \sqrt{1-e^2} (\cos E - e) + f_{12} \sqrt{\frac{1-e^2}{1-e^2 \cos^2 E}} (2 - e^2 - e \cos E) \sin E \right] - f_3 (1 - e \cos E) \cot i \left[\frac{(\cos E - e) \sin \omega}{\sqrt{1-e^2}} + \sin E \cos \omega \right] \right\} \\ \Delta\omega &= \int_{-\alpha}^{\alpha} \left\{ \frac{a^2 f_{12}}{\mu e} \sqrt{\frac{1-e^2}{1-e^2 \cos^2 E}} \sin E [-e(\cos E - e) + (2 - e^2 - e \cos E)] \right\} dE - \\ &\quad - \int_{-\alpha}^{\alpha} \left\{ \frac{a^2}{\mu} f_3 (1 - e \cos E) \cot i \left[\frac{(\cos E - e) \sin \omega}{\sqrt{1-e^2}} + \sin E \cos \omega \right] \right\} dE \end{aligned}$$

With the first integral we obtain:

$$\left| \frac{a^2 f_{12}}{\mu e} \sqrt{1-e^2} \left[\frac{e^2 - 2}{e} \arcsin(e \cos E) - \frac{2}{e} \sqrt{1-e^2 \cos^2 E} \right] \right|_{-\alpha}^{\alpha} = 0$$

The result of the first integral is zero even in case of apoapsis-centred burn, with the limits of the integral $\pi - \alpha$ and $\pi + \alpha$.

Finally, we need to solve the second integral and the result is the same as in case A.1.5.

A.3 Case 3

For the third case, with the in-plane accelerations perpendicular to the major axis of the ellipse, we have $f_1 = \frac{f_{12} \sqrt{1-e^2} \sin E}{1-e \cos E}$ and $f_2 = \frac{f_{12} (\cos E - e)}{1-e \cos E}$.

A.3.1 Semi-major axis $\frac{da}{dE}$

Starting from Eq. 1.2:

$$\frac{da}{dE} = \frac{2a^3}{\mu} \left(f_1 e \sin E + f_2 \sqrt{1-e^2} \right)$$

with steering case 3, we obtain:

$$\frac{da}{dE} = \frac{2a^3}{\mu} \left(\frac{f_{12}\sqrt{1-e^2}\sin E}{1-e\cos E} e \sin E + \frac{f_{12}(\cos E - e)}{1-e\cos E} \sqrt{1-e^2} \right)$$

$$\Delta a = \int_{-\alpha}^{\alpha} \left[\frac{2a^3}{\mu} f_{12}\sqrt{1-e^2} \left(\frac{e - e\cos^2 E + \cos E - e}{1-e\cos E} \right) \right] dE$$

$$\Delta a = \frac{4a^3}{\mu} f_{12}\sqrt{1-e^2} \sin \alpha$$

In order to obtain the secular rates of change we have to divide by the orbit period:

$$\frac{da}{dt} = \frac{1}{2\pi} \sqrt{\frac{\mu}{a^3}} \frac{4a^3}{\mu} f_{12}\sqrt{1-e^2} \sin \alpha$$

$$\frac{da}{dt} = \frac{2f_{12}}{\pi} \sqrt{\frac{a^3}{\mu}(1-e^2)} \sin \alpha$$

In case of apoapsis-centred burn, the limits of the integral are $\pi - \alpha$ and $\pi + \alpha$, and we obtain:

$$\frac{da}{dt} = -\frac{2f_{12}}{\pi} \sqrt{\frac{a^3}{\mu}(1-e^2)} \sin \alpha$$

A.3.2 Eccentricity $\frac{de}{dE}$

Starting from Eq. 1.3:

$$\frac{de}{dE} = \frac{a^2}{\mu} \left[f_1(1-e^2)\sin E + f_2\sqrt{1-e^2}(2\cos E - e - e\cos^2 E) \right]$$

with steering case 3, we obtain:

$$\frac{de}{dE} = \frac{a^2}{\mu} \left[\frac{f_{12}\sqrt{1-e^2}\sin E}{1-e\cos E} (1-e^2)\sin E + \frac{f_{12}(\cos E - e)}{1-e\cos E} \sqrt{1-e^2}(2\cos E - e - e\cos^2 E) \right]$$

$$\Delta e = \int_{-\alpha}^{\alpha} \left[\frac{a^2}{\mu} f_{12}\sqrt{1-e^2} \left(\frac{1 - 3e\cos E + \cos^2 E + 2e^2\cos^2 E - e\cos^3 E}{1-e\cos E} \right) \right] dE$$

$$\Delta e = \frac{a^2}{\mu} f_{12}\sqrt{1-e^2} \int_{-\alpha}^{\alpha} (\cos^2 E - 2e\cos E + 1) dE$$

$$\Delta e = \frac{a^2}{\mu} f_{12}\sqrt{1-e^2} (\alpha + \sin \alpha \cos \alpha - 4e\sin \alpha + 2\alpha)$$

In order to obtain the secular rates of change we have to divide by the orbit period:

$$\frac{de}{dt} = \frac{1}{2\pi} \sqrt{\frac{\mu}{a^3}} \frac{a^2}{\mu} f_{12} \sqrt{1-e^2} (-4e \sin \alpha + 3\alpha + \sin \alpha \cos \alpha)$$

$$\frac{de}{dt} = \frac{f_{12}}{2\pi} \sqrt{\frac{a}{\mu}} (1-e^2) (-4e \sin \alpha + 3\alpha + \sin \alpha \cos \alpha)$$

In case of apoapsis-centred burn, the limits of the integral are $\pi - \alpha$ and $\pi + \alpha$, and we obtain:

$$\frac{de}{dt} = \frac{f_{12}}{2\pi} \sqrt{\frac{a}{\mu}} (1-e^2) (4e \sin \alpha + 3\alpha + \sin \alpha \cos \alpha)$$

A.3.3 Inclination $\frac{di}{dE}$

We reach the same result as in case 1 because it is not a function of f_1 or f_2 . See A.1.3.

A.3.4 RAAN $\frac{d\Omega}{dE}$

We reach the same result as in case 1 because it is not a function of f_1 or f_2 . See A.1.4.

A.3.5 Argument of periapsis $\frac{d\omega}{dE}$

Starting from Eq. 1.6:

$$\begin{aligned} \frac{d\omega}{dE} = \frac{a^2}{\mu} \left\{ \frac{1}{e} \left[-f_1 \sqrt{1-e^2} (\cos E - e) + f_2 (2 - e^2 - e \cos E) \sin E \right] - \right. \\ \left. - f_3 (1 - e \cos E) \cot i \left[\frac{(\cos E - e) \sin \omega}{\sqrt{1-e^2}} + \sin E \cos \omega \right] \right\} \end{aligned}$$

with steering case 3, we obtain:

$$\begin{aligned} \frac{d\omega}{dE} = \frac{a^2}{\mu} \left\{ \frac{1}{e} \left[-\frac{f_{12} \sqrt{1-e^2} \sin E}{1 - e \cos E} \sqrt{1-e^2} (\cos E - e) + \frac{f_{12} (\cos E - e)}{1 - e \cos E} (2 - e^2 - \right. \right. \\ \left. \left. - e \cos E) \sin E \right] - f_3 (1 - e \cos E) \cot i \left[\frac{(\cos E - e) \sin \omega}{\sqrt{1-e^2}} + \sin E \cos \omega \right] \right\} \end{aligned}$$

$$\begin{aligned} \Delta\omega = \int_{-\alpha}^{\alpha} \frac{a^2}{\mu} \frac{f_{12}}{e} \left[\frac{\sin E (\cos E - e) (e^2 - 1 + 2 - e^2 - e \cos E)}{1 - e \cos E} \right] dE - \\ - \int_{-\alpha}^{\alpha} \left\{ \frac{a^2}{\mu} f_3 (1 - e \cos E) \cot i \left[\frac{(\cos E - e) \sin \omega}{\sqrt{1-e^2}} + \sin E \cos \omega \right] \right\} dE \end{aligned}$$

With the first integral we obtain:

$$|\sin E(\cos E - e)|_{-\alpha}^{\alpha} = 0$$

The result of the first integral is zero even in case of apoapsis-centred burn, with the limits of the integral $\pi - \alpha$ and $\pi + \alpha$.

Finally, we need to solve the second integral and the result is the same as in case A.1.5.

A.4 Case 4

For the fourth case, with the in-plane accelerations parallel to the major axis of the ellipse, we have $f_1 = \frac{f_{12}(\cos E - e)}{1 - e \cos E}$ and $f_2 = \frac{-f_{12}\sqrt{1 - e^2} \sin E}{1 - e \cos E}$.

A.4.1 Semi-major axis $\frac{da}{dE}$

Starting from Eq. 1.2:

$$\frac{da}{dE} = \frac{2a^3}{\mu} \left(f_1 e \sin E + f_2 \sqrt{1 - e^2} \right)$$

with steering case 4, we obtain:

$$\begin{aligned} \frac{da}{dE} &= \frac{2a^3}{\mu} \left(\frac{f_{12}(\cos E - e)}{1 - e \cos E} e \sin E + \frac{-f_{12}\sqrt{1 - e^2} \sin E}{1 - e \cos E} \sqrt{1 - e^2} \right) \\ \Delta a &= \int_{-\alpha}^{\alpha} \left[\frac{2a^3}{\mu} f_{12} \left(\frac{e \cos E \sin E - e^2 \sin E - \sin E + e^2 \sin E}{1 - e \cos E} \right) \right] dE \\ \Delta a &= -\frac{2a^3}{\mu} f_{12} \int_{-\alpha}^{\alpha} \sin E dE = 0 \end{aligned}$$

In case of apoapsis-centred burn, the limits of the integral are $\pi - \alpha$ and $\pi + \alpha$, and we obtain the same result.

A.4.2 Eccentricity $\frac{de}{dE}$

Starting from Eq. 1.3:

$$\frac{de}{dE} = \frac{a^2}{\mu} \left[f_1(1 - e^2) \sin E + f_2 \sqrt{1 - e^2} (2 \cos E - e - e \cos^2 E) \right]$$

with steering case 4, we obtain:

$$\frac{de}{dE} = \frac{a^2}{\mu} \left[\frac{f_{12}(\cos E - e)}{1 - e \cos E} (1 - e^2) \sin E + \frac{-f_{12}\sqrt{1 - e^2} \sin E}{1 - e \cos E} \sqrt{1 - e^2} (2 \cos E - e - e \cos^2 E) \right]$$

$$\Delta e = \int_{-\alpha}^{\alpha} \left[\frac{a^2}{\mu} f_{12} (1 - e^2) \left(\frac{\cos E \sin E - 2 \cos E \sin E + e \cos^2 E \sin E}{1 - e \cos E} \right) \right] dE$$

$$\Delta e = -\frac{a^2}{\mu} f_{12} (1 - e^2) \int_{-\alpha}^{\alpha} \cos E \sin E dE = 0$$

In case of apoapsis-centred burn, the limits of the integral are $\pi - \alpha$ and $\pi + \alpha$, and we obtain the same result.

A.4.3 Inclination $\frac{di}{dE}$

We reach the same result as in case 1 because it is not a function of f_1 or f_2 . See A.1.3.

A.4.4 RAAN $\frac{d\Omega}{dE}$

We reach the same result as in case 1 because it is not a function of f_1 or f_2 . See A.1.4.

A.4.5 Argument of periapsis $\frac{d\omega}{dE}$

Starting from Eq. 1.6:

$$\begin{aligned} \frac{d\omega}{dE} = \frac{a^2}{\mu} \left\{ \frac{1}{e} \left[-f_1 \sqrt{1 - e^2} (\cos E - e) + f_2 (2 - e^2 - e \cos E) \sin E \right] - \right. \\ \left. - f_3 (1 - e \cos E) \cot i \left[\frac{(\cos E - e) \sin \omega}{\sqrt{1 - e^2}} + \sin E \cos \omega \right] \right\} \end{aligned}$$

with steering case 4, we obtain:

$$\begin{aligned} \frac{d\omega}{dE} = \frac{a^2}{\mu} \left\{ \frac{1}{e} \left[-\frac{f_{12}(\cos E - e)}{1 - e \cos E} \sqrt{1 - e^2} (\cos E - e) + \frac{-f_{12}\sqrt{1 - e^2} \sin E}{1 - e \cos E} (2 - e^2 - \right. \right. \\ \left. \left. - e \cos E) \sin E \right] - f_3 (1 - e \cos E) \cot i \left[\frac{(\cos E - e) \sin \omega}{\sqrt{1 - e^2}} + \sin E \cos \omega \right] \right\} \end{aligned}$$

$$\Delta\omega = \int_{-\alpha}^{\alpha} \frac{a^2}{\mu} \frac{f_{12}}{e} \sqrt{1-e^2} \left(\frac{-2 + 3e \cos E + \cos^2 E - e^2 \cos^2 E - e \cos^3 E}{1 - e \cos E} \right) dE -$$

$$- \int_{-\alpha}^{\alpha} \left\{ \frac{a^2}{\mu} f_3 (1 - e \cos E) \cot i \left[\frac{(\cos E - e) \sin \omega}{\sqrt{1-e^2}} + \sin E \cos \omega \right] \right\} dE$$

With the first integral we obtain:

$$\Delta\omega = \frac{a^2}{\mu} \frac{f_{12}}{e} \sqrt{1-e^2} \int_{-\alpha}^{\alpha} (-2 + e \cos E + \cos^2 E) dE =$$

$$= \frac{a^2}{\mu} \frac{f_{12}}{e} \sqrt{1-e^2} (2e \sin \alpha - 3\alpha + \sin \alpha \cos \alpha)$$

The second integral give the same result of case A.1.5. Finally, by summing the two integrals and dividing by the orbit period, we obtain:

$$\frac{d\omega}{dt} = \frac{1}{2\pi} \sqrt{\frac{a}{\mu}} \left\{ f_{12} \frac{\sqrt{1-e^2}}{e} (2e \sin \alpha - 3\alpha + \sin \alpha \cos \alpha) - \right.$$

$$\left. - f_3 \frac{\sin \omega}{\sqrt{1-e^2}} \cot i [2 \sin \alpha (1 + e^2) - 3e\alpha - e \sin \alpha \cos \alpha] \right\}$$

In case of apoapsis-centred burn, the limits of the integral are $\pi - \alpha$ and $\pi + \alpha$, and we obtain:

$$\frac{d\omega}{dt} = \frac{1}{2\pi} \sqrt{\frac{a}{\mu}} \left\{ f_{12} \frac{\sqrt{1-e^2}}{e} (-2e \sin \alpha - 3\alpha + \sin \alpha \cos \alpha) - \right.$$

$$\left. - f_3 \frac{\sin \omega}{\sqrt{1-e^2}} \cot i [-2 \sin \alpha (1 + e^2) - 3e\alpha - e \sin \alpha \cos \alpha] \right\}$$

Bibliography

- [1] Oliver Schütze, Massimiliano Vasile, Oliver Junge, Michael Dellnitz, Dario Izzo. Designing optimal low-thrust gravity-assist trajectories using space pruning and a multi-objective approach. *Engineering Optimization*, 2009.
- [2] Theodore N. Edelbaum. Propulsion requirements for controllable satellites. *United Aircraft Corp.*, 1961.
- [3] J.E. Polk, R.Y. Kakuda, J.R. Anderson, J.R. Brophy, V.K. Rawlin, M.J. Patterson, J. Sovey, J. Hamley. Performance of the NSTAR Ion Propulsion System on the Deep Space One Mission. *American Institute of Aeronautics and Astronautics*, 2001.
- [4] George R. Schmidt, Michael J. Patterson, Scott W. Benson. The NASA Evolutionary Xenon Thruster (NEXT): the next stop for U.S. Deep Space propulsion. *IAC 2008 59th International Astronautical Congress*, 2008.
- [5] M. Manente, F. Trezzolani, A. Selmo, E. Fantino, G. Mistè, E. Toson, D. Pavarin. A low-cost Helicon Propulsion System to boost small satellite missions. *IAC 2017 68th International Astronautical Congress*, 2017.
- [6] Arthur E. Bryson, Yu-Chi Ho. *Applied Optimal Control*. Taylor and Francis Group, 1975.
- [7] Bruce A. Conway. *Spacecraft Trajectory Optimization*. Cambridge University Press, 2010.
- [8] Elena Fantino and Roberto Castelli. Efficient design of direct low-energy transfers in multi-moon systems. *Celestial Mechanics and Dynamical Astronomy*, 2016.
- [9] James E. Pollard. Simplified Approach for Assessment of Low-Thrust Elliptical Orbit Transfers. *The Aerospace Corporation*, 1997.

-
- [10] James E. Pollard. Simplified Analysis of Low-Thrust Orbital Maneuvers. *The Aerospace Corporation*, 2000.
- [11] E.G.C.Burt. On Space Manoeuvres With Continuous Thrust. *Planet. Space Sci. Vol.15*, 1967.
- [12] David H. Atkinson et al. Entry Probe Missions to the Giant Planets. *AAS/Division for Planetary Sciences Meeting Abstracts 41*, 2009.
- [13] Wang Sang Koon, Martin W. Lo, Jerrold E. Marsden, Shane D. Ross. Constructing a Low Energy Transfer Between Jovian Moons. *Celestial Mechanics and Dynamical Astronomy*, 2001.
- [14] Andrea Viale. Low-energy tour of the Galilean moons. *Master degree thesis at Università degli Studi di Padova*, 2016.
- [15] Roger R. Bate, Donald D. Mueller, Jerry E. White. *Fundamentals of Astrodynamics*. Dover Publications, Inc, 1971.
- [16] Elena Fantino, Roberto M. Flores, Ashraf N. Al-Khateeb. Efficient Two-Body Approximations of Impulsive Transfers between Halo Orbits. *IAC 2018 69th International Astronautical Congress*, 2018.